CHAPTER 3
RESULTS AND DISCUSSION

The FI-spectrophotometric method for speciation of selenite and selenate in waters was developed. The experimental conditions considered were evaluated by univariate optimization method. The proposed method was applied to water samples collected in Chiang Mai Province.

3.1 Preliminary Study of Absorption Spectra

Preliminary study showed that selenite reacted with iodide in acidic medium and followed by rhodamine B resulting in a purple complex . The absorbance of the complex and reagent solutions was scanned between 500 and 800 nm as shown in Figure 3.1.

Figure 3.1 The absorption spectra of reagent and complex solutions: (a) the reagent solution against water as blank solution and (b) the complex solution against reagent as blank solution

The solution of ion-association complex presented maximum absorption at 587 nm while that of the reagent solution showed maximum absorption at 526 nm and low absorption at about 587 nm under the same experimental conditions which means that positive peak at 587 nm can be measured. In this study, a spectrophotometric procedure was proposed for determining selenite using rhodamine B as complexing agent.

3.2 Optimization of the Flow System

The analytical parameters of the flow system were optimized to achieve the best analytical characteristics, such as sensitivity and speed, by the univariate method. The fixed parameters (by random) were shown in Table 3.1.

Table 3.1 Fixed experimental parameters for study of optimum conditions.

Parameter	Information
HCl concentration (M)	0.10
KI concentration (M)	0.20
NaOAc concentration (M)	0.10
PVA concentration (% w/v)	1.0
RhB concentration (M)	1.6×10^{-4}
Flow rate of sample solution (ml/min)	1.0
Flow rate of HCl solution (ml/min)	1.0
Flow rate of KI solution (ml/min)	1.0
Size of mixing tubing (tygon) (cm i.d.)	0.076
Size of mixing tubing (PTFE) (cm i.d.)	0.086
Length of mixing tubing (cm)	100
Size of test tube for mixing coil (cm)	1.9
Injection volume (μl)	150
Chart speed (cm/h)	10
Sensitivity (mV/cm)	4

3.2.1 Effect of wavelength

Optimization of the experimental conditions was started with optimum wavelength for selenite determination. A comparative study of the absorption spectrum of the ion-association complex was carried out by FI method with spectrophotometric detection using the experimental conditions as shown in Table 3.1. The optimum wavelength was investigated over the range 575 to 630 nm by introducing 0.5 ppm of selenite standard solution into the proposed FI system (Figure 2.1). The FIA signals in the form of peak height obtained at various operating wavelengths were shown in Table 3.2. The absorption spectrum was obtained by plotting peak height against various detector wavelengths as shown in Figure 3.2.

Table 3.2 Peak height at various wavelengths.

Wavelength (nm)	Peak height					
	Blank		Analyte		Net	
	cm	mV	cm	mV	cm	mV
575	3.73	14.92	3.93	15.72	0.20	0.80
580	2.82	11.28	3.32	13.28	0.50	2.00
585	1.83	7.32	3.01	12.04	1.18	4.72
590	1.05	4.20	2.37	9.48	1.32	5.28
595	0.55	2.20	1.55	6.20	1.00	4.00
600	0.33	1.32	0.95	3.80	0.62	2.48
605	0.17	0.68	0.60	2.40	0.43	1.72
610	0.10	0.40	0.39	1.56	0.29	1.16
615	0.10	0.40	0.32	1.28	0.22	0.88
620	0.05	0.20	0.20	0.80	0.15	0.60
625	0.05	0.20	0.15	0.60	0.10	0.40
630	0.00	0.00	0.10	0.40	0.10	0.40

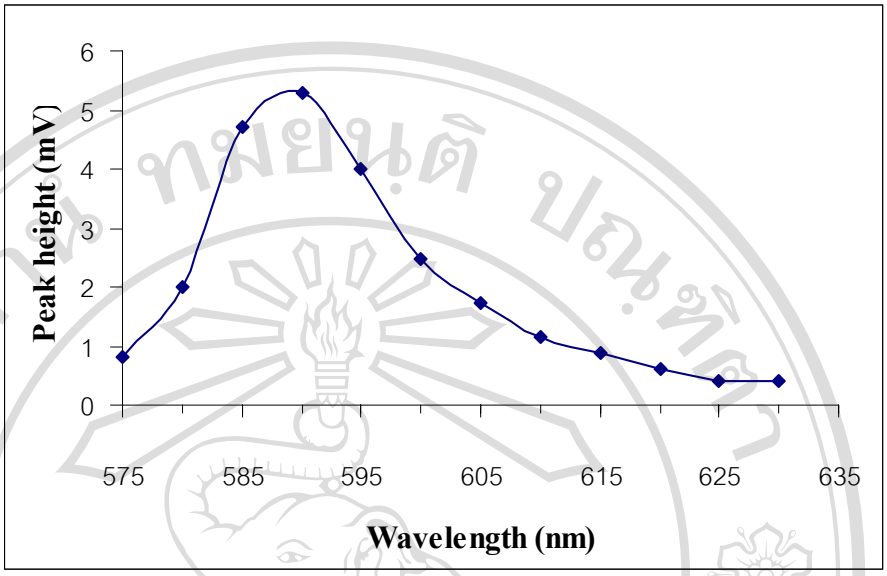

Figure 3.2 Relationship between peak height and various wavelengths.

It was seen that the maximum peak height was observed at 590 nm. Therefore, this wavelength was chosen as optimum condition for further FIA measurements in order to assess the best sensitivity.

3.2.2 Effect of HCl concentration

In this experiment, hydrochloric acid, donor solution, was chosen for the oxidation reaction as mentioned. The oxidation of iodide with selenite can occur in weak acid medium that is this reaction are acidity dependent. Therefore it is essential to investigate the optimum acidity for the reaction. The effect of HCl concentration on peak height from various concentrations of selenite (0.1 to 0.5 ppm) was carried out by varying differrent concentrations of HCl from 0.20 to 0.40 M. The results were shown in Table 3.3 and Figures 3.3 and 3.4. From the experimental results, the optimum HCl concentration was 0.25 M since it provided highest sensitivity with a good linearity of calibration curve. Thus, the oxidation reaction occurred completely in 0.25 M hydrochloric acid medium which was chosen for subsequent experiments.

Table 3.3 Effect of HCl concentration on peak height.

[Se(IV)] (ppm)	Peak height (mV) obtained for [HCl] (M)				
	0.20	0.25	0.30	0.35	0.40
0.1	0.12	0.40	0.32	0.28	0.20
0.2	0.48	0.68	0.52	0.48	0.48
0.3	0.60	1.00	0.80	0.88	0.80
0.4	0.80	1.28	1.08	1.12	0.92
0.5	0.92	1.52	1.28	1.40	1.20
Slope (mV/ppm)	1.93	3.02	2.56	2.83	2.42
Correlation coefficient	0.9742	0.9943	0.9965	0.9947	0.9908

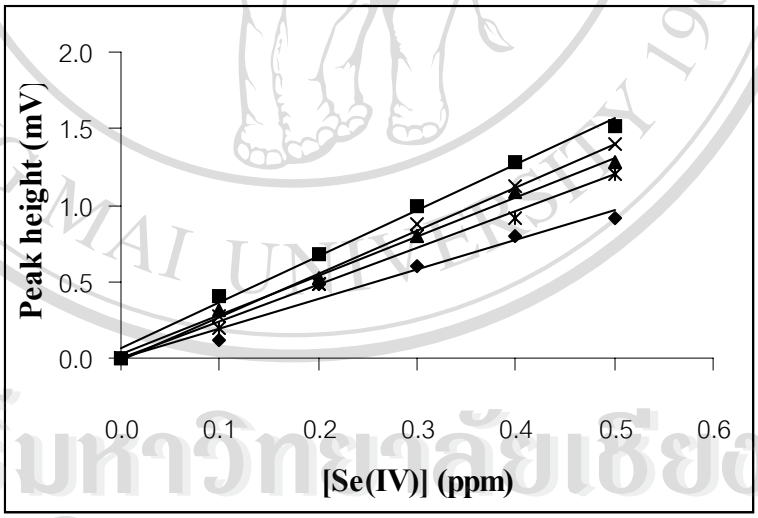

Figure 3.3 Effect of HCl concentration on peak height: (a) 0.20; (b) 0.25; (c) 0.30; (d) 0.35; and (e) 0.40 M.

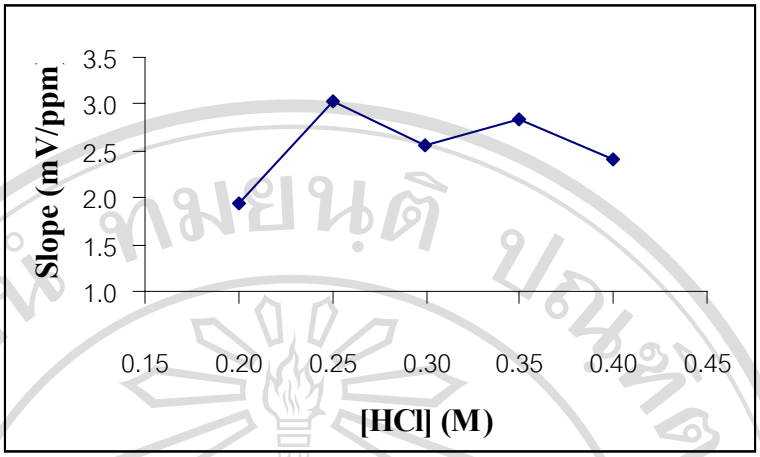

Figure 3.4 Relationship between slope and HCl concentration.

3.2.3 Effect of KI concentration

Optimization of KI concentration, Table 3.4 and Figure 3.5 showed peak height obtained from varying the KI concentration ranging from 0.19 to 0.27 M where as Figure 3.6 showed a relationship between slope of calibration graph and various KI concentrations.

Table 3.4 Effect of KI concentration on peak height.

[Se(IV)] (ppm)	Peak height (mV) obtained for [KI] (M)				
	0.19	0.21	0.23	0.25	0.27
0.1	0.20	0.32	0.40	0.40	0.28
0.2	0.32	0.68	0.92	0.72	0.48
0.3	0.60	1.12	1.32	1.28	0.72
0.4	0.72	1.40	2.08	1.48	1.12
0.5	0.92	1.72	2.40	2.12	1.48
Slope (mV/ppm)	1.84	3.51	4.98	4.11	2.90
Correlation coefficient	0.9914	0.9967	0.9906	0.9869	0.9847

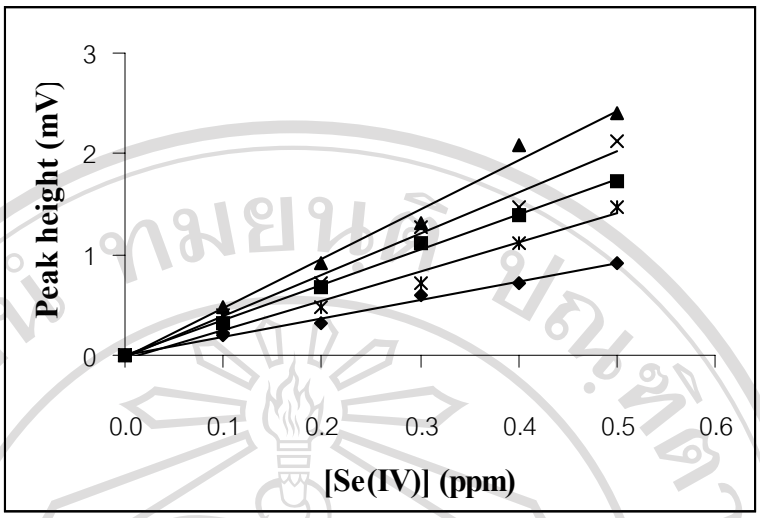

Figure 3.5 Effect of KI concentration on peak height: (a) 0.19; (b) 0.21; (c) 0.23; (d) 0.25; and (e) 0.27 M.

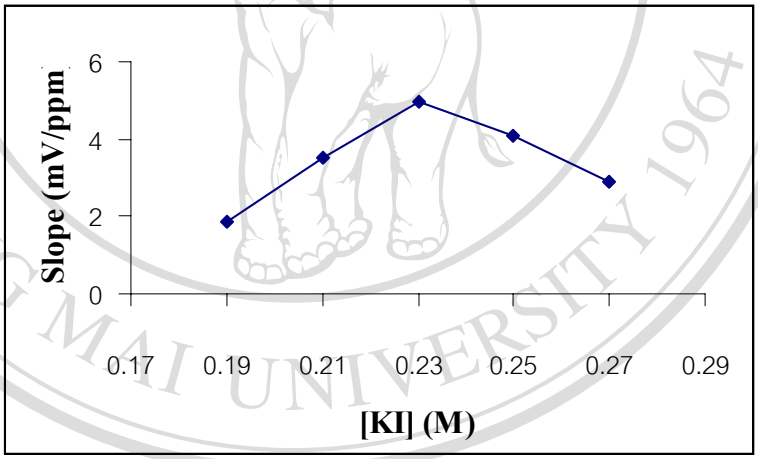

Figure 3.6 Relationship between slope and KI concentration.

Figure 3.6 indicated that the sensitivity increased rapidly with increasing KI concentration up to 0.23 M and the sensitivity decreased rapidly when the concentration of KI was greater than 0.23 M. Thus 0.23 M of KI concentration was chosen as optimum concentration for subsequent experiments since it provided the highest sensitivity for this investigation.

3.2.4 Effect of NaOAc concentration

Effect of NaOAc concentration was studied because concentration of NaOAc can affect the complexation reaction. The concentration of NaOAc was varied over the range 0.05 to 0.25 M.

Table 3.5 Effect of NaOAc concentration on peak height.

[Se(IV)] (ppm)	Peak height (mV) obtained for [NaOAc] (M)				
	0.05	0.10	0.15	0.20	0.25
0.1	0.40	0.52	0.60	0.52	0.48
0.2	0.88	0.92	1.00	0.92	0.80
0.3	1.20	1.40	1.48	1.52	1.48
0.4	1.52	1.88	1.92	1.88	1.80
0.5	1.92	2.48	2.32	2.20	2.12
Slope (mV/ppm)	3.79	4.84	4.58	4.48	4.35
Correlation coefficient	0.9958	0.9970	0.9964	0.9918	0.9880

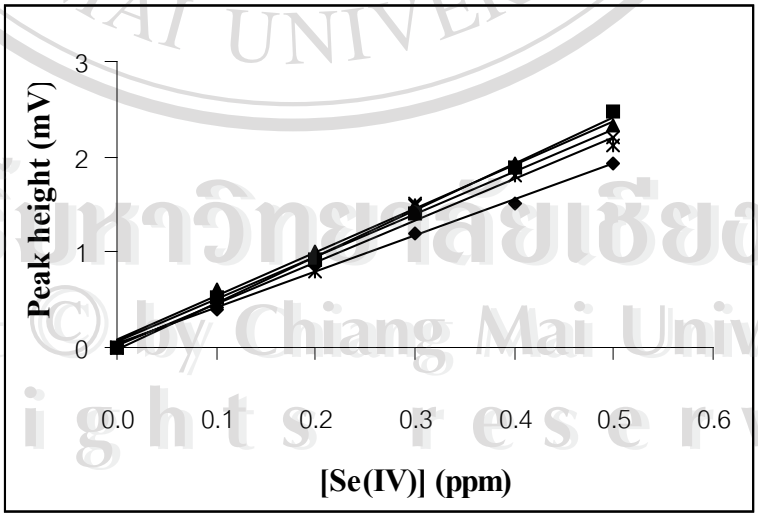

Figure 3.7 Effect of NaOAc concentration on peak height: (a) 0.05; (b) 0.10; (c) 0.15; (d) 0.20; and (e) 0.25 M.

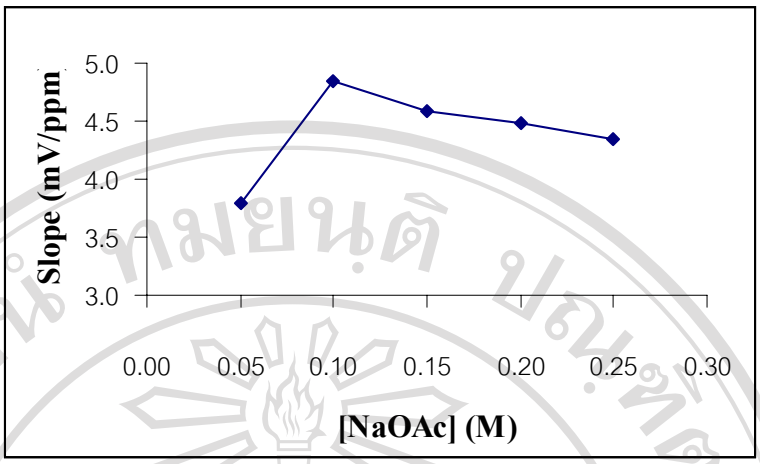

Figure 3.8 Relationship between slope and NaOAc concentration.

The results obtained as shown in Table 3.5 and Figures 3.7 and 3.8 indicated that the slope of the calibration curve increased when the concentration of NaOAc increased up to 0.10 M. Afterwards, the slope decreased slightly when the concentration of NaOAc reached 0.25 M. It was showed that the optimum concentration of NaOAc is 0.10 M.

3.2.5 Effect of PVA concentration

The PVA solution was added as solubilizer to prevent precipitation in complexation reaction. Effect of various PVA concentrations on peak height were investigated by varying the concentration of PVA in the range of 0.5 to 2.5% w/v. The results obtained were exhibited in Table 3.6 and Figures 3.9 and 3.10. From the experimental results, the slope of calibration curve over the range 0.1 to 0.5 ppm selenite increased with PVA concentration up to 1.0% w/v, followed by a slight decrease in peak height at the concentration of 1.5%. Afterwards, the slope of calibration curve decreased rapidly when the concentration increased up to 2.0% and decreased slightly when the PVA concentration reached 2.5%. The results indicated that the highest sensitivity was obtained when the concentration of PVA was 1.0% w/v.

Table 3.6 Effect of PVA concentration on peak height.

[Se(IV)] (ppm)	Peak height (mV) obtained for [PVA] (% w/v)				
	0.5	1.0	1.5	2.0	2.5
0.1	0.40	0.48	0.52	0.28	0.32
0.2	0.72	0.88	0.88	0.72	0.72
0.3	0.88	1.48	1.52	1.08	1.00
0.4	1.28	1.92	2.00	1.40	1.48
0.5	1.52	2.52	2.32	1.92	1.68
Slope (mV/ppm)	2.97	5.00	4.76	3.80	3.47
Correlation coefficient	0.9895	0.9968	0.9933	0.9941	0.9932

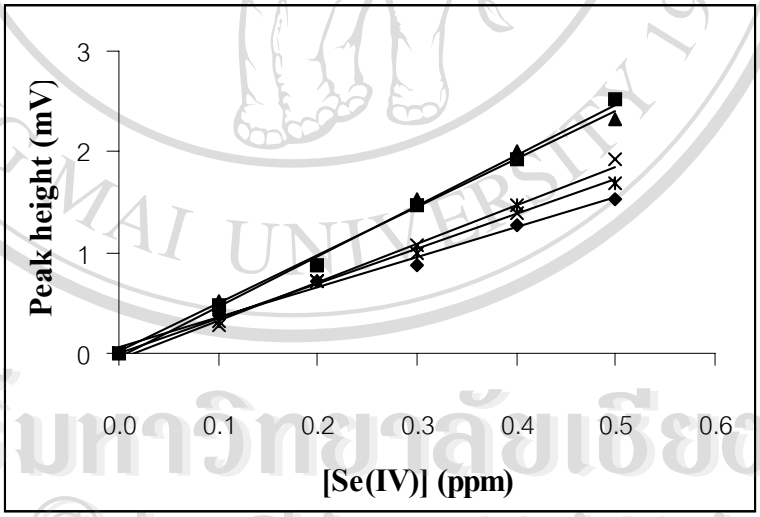

Figure 3.9 Effect of PVA concentration on peak height: (a) 0.1; (b) 0.5; (c) 1.0; (d) 1.5; and (e) 2.0% w/v.

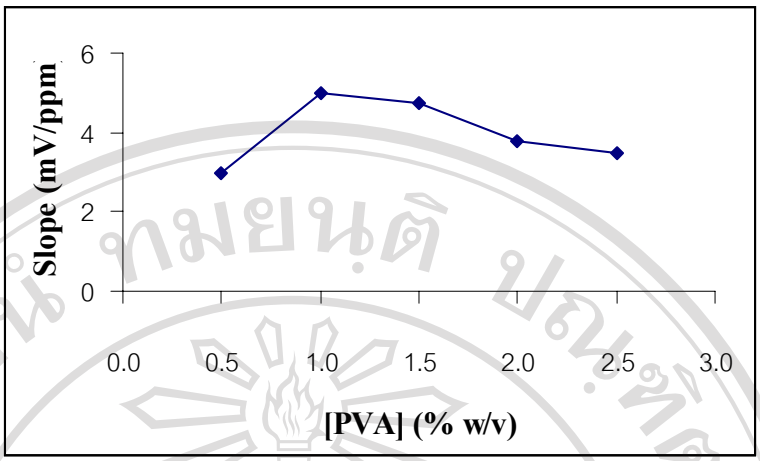

Figure 3.10 Relationship between slope and PVA concentration.

3.2.6 Effect of rhodamine B concentration

Effect of concentration of rhodamine B was investigated at varying concentrations (1.6 to 2.4×10^{-4} M) and the results obtained are shown in Table 3.7 and Figures 3.11 and 3.12.

Table 3.7 Effect of rhodamine B concentration on peak height.

[Se(IV)] (ppm)	Peak height (mV) obtained for [RhB] (× 10^{-4} M)				
	1.6	1.8	2.0	2.2	2.4
0.1	0.52	0.68	0.88	0.60	0.68
0.2	0.92	1.28	1.60	1.48	1.28
0.3	1.48	2.00	2.60	2.80	2.08
0.4	2.20	2.72	3.28	3.12	2.80
0.5	2.52	3.48	4.20	4.08	3.20
Slope (mV/ppm)	5.20	6.92	8.34	8.36	6.62
Correlation coefficient	0.9922	0.9986	0.9984	0.9837	0.9943

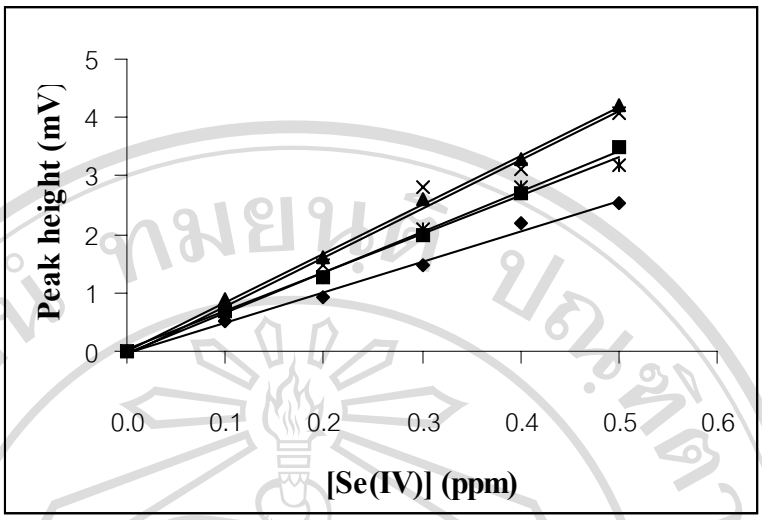

Figure 3.11 Effect of rhodamine B concentration on peak height: (a) 1.6; (b) 1.8; (c) 2.0; (d) 2.2; and (e) 2.4×10^{-4} M.

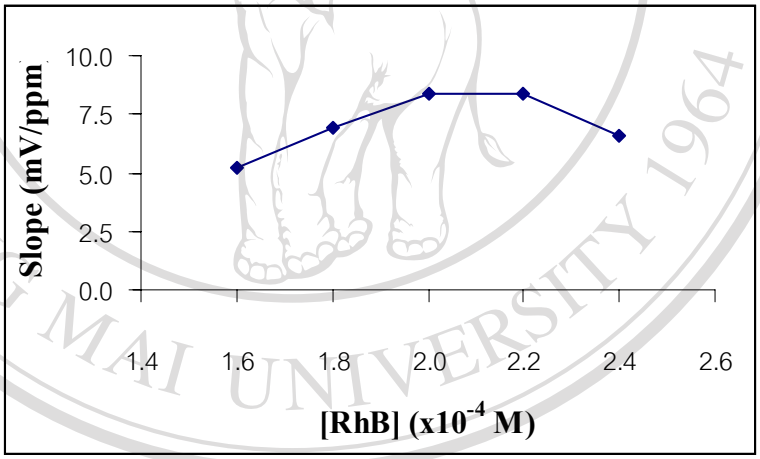

Figure 3.12 Relationship between slope and rhodamine B concentration.

The results indicated that the optimum sensitivity is between 2.0 and 2.2×10^{-4} M, but the peak height or the slope of the calibration curve for selenite obtained by using 2.0×10^{-4} M rhodamine B was slightly greater than those obtained by using 2.2×10^{-4} M rhodamine B. Therefore, the appropriate concentraiton was 2.0×10^{-4} M due to high sensitivity with better linearity of calibration curve.

3.2.7 Effect of flow rate of sample solution

In the reverse flow injection system, the solution of sample and/or standard solution was pumped into three-line manifold via peristaltic pump through the 0.152 cm inside diameter tygon tubing. The flow rate of sample and/or standard solution can affect the dispersion and thus, sensitivity. Therefore it is necessary to investigate the effect of flow rate on peak height or sensitivity by varying the flow rate from 0.7 to 1.9 ml/min and fixing the flow rate of HCl and KI solutions at 1.0 ml/min. The results were summarized in Tables 3.8-3.9 and Figures 3.13-3.15. The results indicated that the slope of standard calibration curve increased when the flow rate of sample and/or standard solution decreased (from 1.0 up to 1.9 ml/min). The highest slope was obtained when the flow rate equal 1.0 ml/min. It can be seen that high sample throughput (low t_{base}) was obtained when the flow rate equal or greater than 1.0 ml/min. Thus a flow rate of 1.0 ml/min was chosen as optimum flow rate in order to obtain highest sensitivity with good linearity of calibration curve and reasonable sample throughput.

Table 3.8 Effect of flow rate of sample solution on peak height.

[Se(IV)] (ppm)	Peak height (mV) obtained for flow rate of sample (ml/min)				
	0.7	1.0	1.3	1.6	1.9
0.1	0.64	0.88	0.72	0.72	0.60
0.2	1.40	1.60	1.60	1.32	1.00
0.3	1.80	2.68	2.28	2.08	1.52
0.4	2.48	3.20	3.12	2.80	2.40
0.5	3.40	4.12	3.52	3.32	2.88
Slope (mV/ppm)	6.55	8.18	7.28	6.74	5.80
Correlation coefficient	0.9909	0.9953	0.9924	0.9979	0.9889

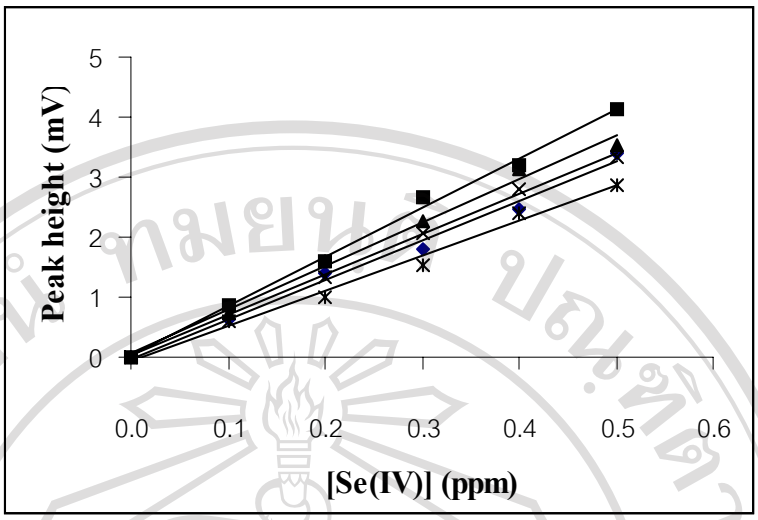

Figure 3.13 Effect of flow rate of sample solution on peak height: (a) 0.7; (b) 1.0; (c) 1.3; (d) 1.6; and (e) 1.9 ml/min.

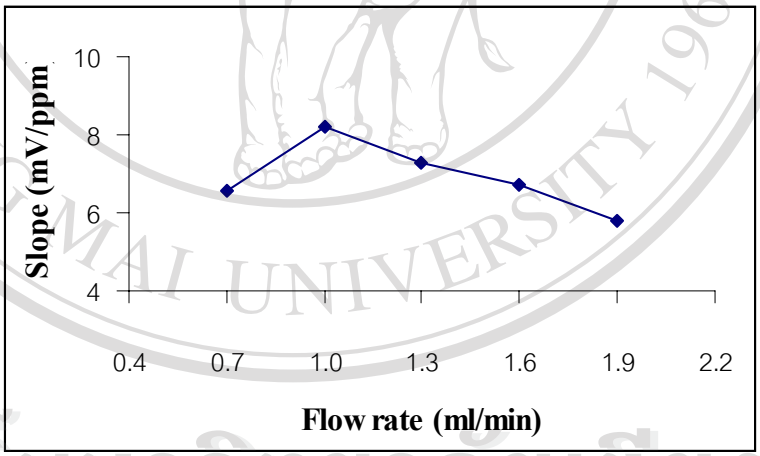

Figure 3.14 Relationship between slope and flow rate of sample solution.

Table 3.9 Analytical characteristics at various flow rates of sample solution.

Flow rate of sample (ml/min)	Peak width (cm)	t_{base} (s)	Sample/h
0.7	0.42	182	19
1.0	0.33	144	25
1.3	0.33	144	25
1.6	0.33	144	25
1.9	0.33	144	25

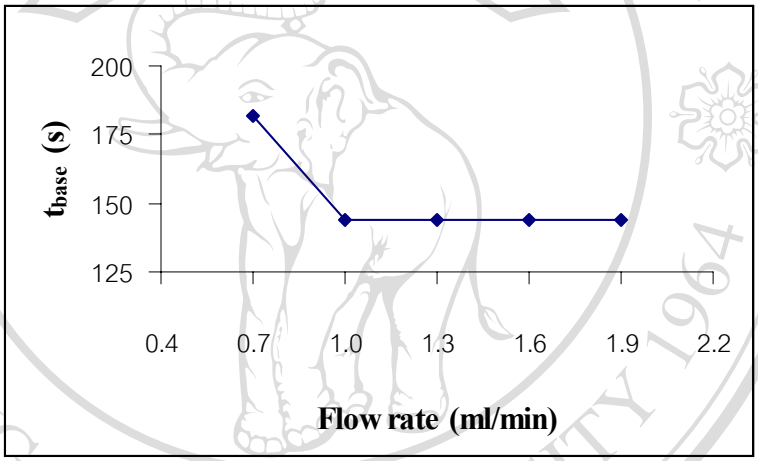

Figure 3.15 Relationship between t_{base} and flow rate of sample solution.

3.2.8 Effect of flow rate of HCl solution

The HCl stream was merged with the sample stream via the same pump. Optimization of flow rate of HCl solution was examined by varying the flow rate of HCl solution in the range of 0.7 to 1.9 ml/min. Tables 3.10-3.11 and Figures 3.16-3.18 showed that the sensitivity decreased when the flow rate of HCl solution increased (from 1.0 up to 1.9 ml/min). It can be observed that higher t_{base} was obtained when the flow rate was 0.7 ml/min. The highest sensitivity and adequate sample throughput were obtained when the flow rate was 1.0 ml/min. Therefore the optimum flow rate chosen for this experiment was 1.0 ml/min.

Table 3.10 Effect of flow rate of HCl solution on peak height.

[Se(IV)] (ppm)	Peak height (mV) obtained for flow rate of HCl (ml/min)				
	0.7	1.0	1.3	1.6	1.9
0.1	0.80	0.88	0.56	0.40	0.32
0.2	1.60	1.68	1.12	0.92	0.60
0.3	2.40	2.68	1.72	1.48	0.92
0.4	2.92	3.48	2.20	1.68	1.28
0.5	3.48	4.00	2.88	2.20	1.72
Slope (mV/ppm)	7.02	8.23	5.69	4.40	3.37
Correlation coefficient	0.9916	0.9938	0.9988	0.9900	0.9939

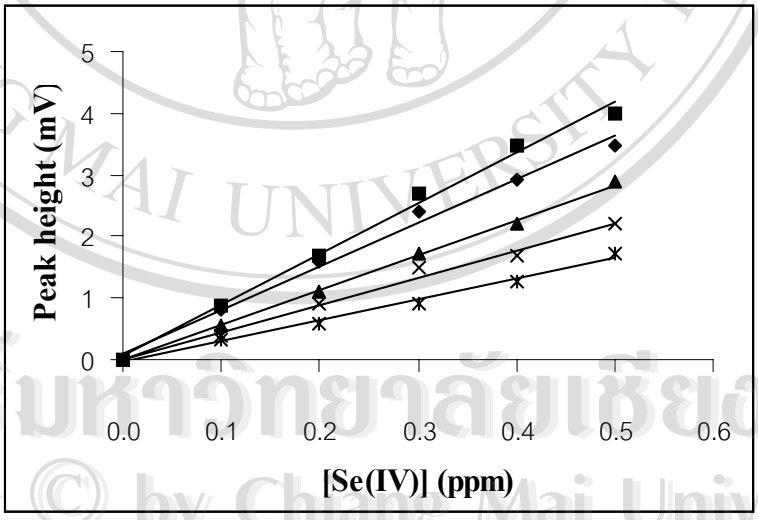

Figure 3.16 Effect of flow rate of HCl solution on peak height: (a) 0.7; (b) 1.0; (c) 1.3 (d) 1.6; and (e) 1.9 ml/min.

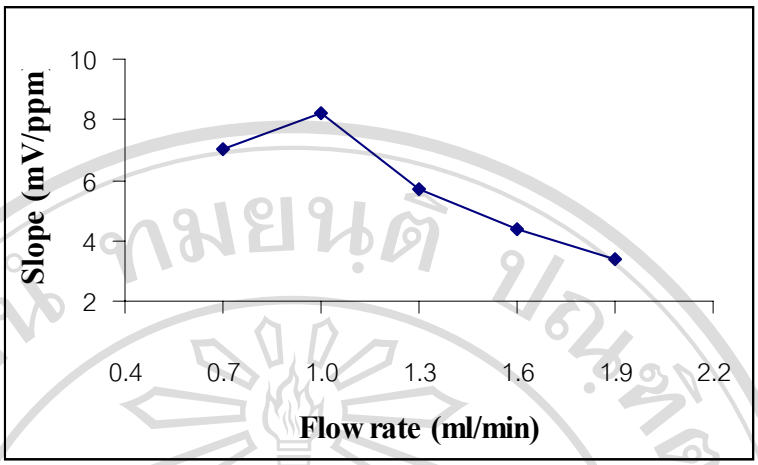

Figure 3.17 Relationship between slope and flow rate of HCl solution.

Table 3.11 Analytical characteristics at various flow rates of HCl solution.

Flow rate of HCl (ml/min)	Peak width (cm)	t_{base} (s)	Sample/h
0.7	0.37	159	23
1.0	0.31	132	27
1.3	0.31	132	27
1.6	0.31	132	27
1.9	0.31	132	27

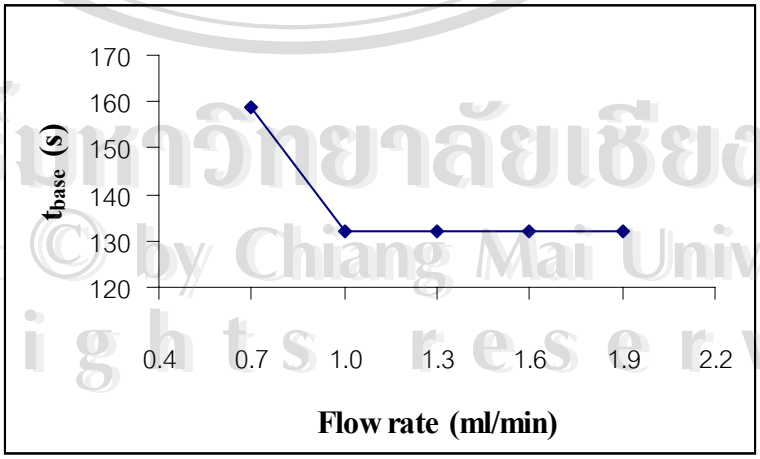

Figure 3.18 Relationship between t_{base} and flow rate of HCl solution.

3.2.9 Effect of flow rate of KI solution

The flow rate of KI solution plays an important role in the system since it affects the dispersion in flow channel. The effect was studied in the range of 0.7 to 1.9 ml/min (Tables 3.12-3.13 and Figures 3.19-3.21).

Table 3.12 Effect of flow rate of KI solution on peak height.

[Se(IV)] (ppm)	Peak height (mV) obtained for flow rate of KI (ml/min)				
	0.7	1.0	1.3	1.6	1.9
0.1	0.60	0.92	0.80	0.48	0.20
0.2	1.28	1.60	1.68	0.72	0.48
0.3	1.68	2.88	2.60	1.12	0.80
0.4	2.20	3.40	3.28	1.48	0.92
0.5	3.12	3.92	3.92	1.72	1.20
Slope (mV/ppm)	5.94	8.09	7.99	3.43	2.42
Correlation coefficient	0.9884	0.9826	0.9959	0.9921	0.9908

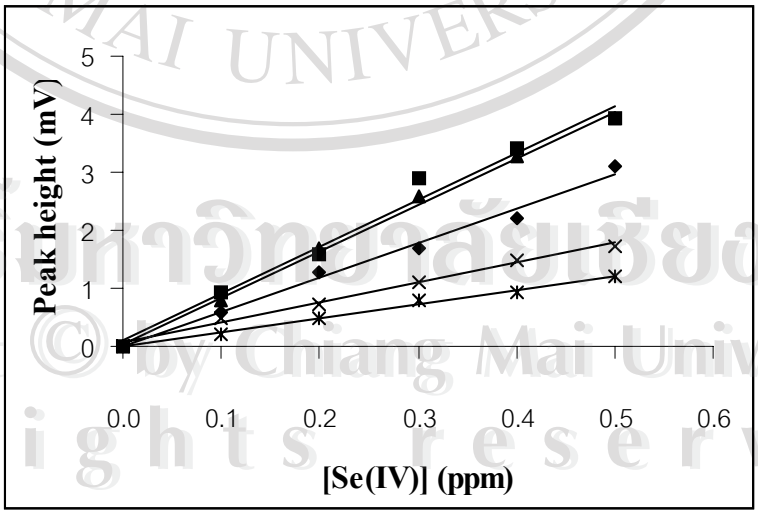

Figure 3.19 Effect of flow rate of KI solution on peak height: (a) 0.7; (b) 1.0; (c) 1.3; (d)1.6 and (e) 1.9 ml/min.

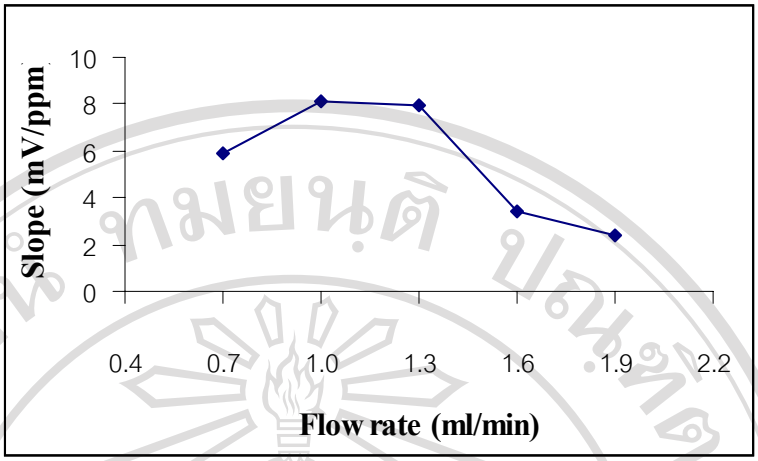

Figure 3.20 Relationship between slope and flow rate of KI solution.

Table 3.13 Analytical characteristics at various flow rates of KI solution.

Flow rate of KI (ml/min)	Peak width (cm)	t_{base} (s)	Sample/h
0.7	0.36	154	23
1.0	0.36	154	23
1.3	0.29	126	28
1.6	0.29	126	28
1.9	0.29	126	28

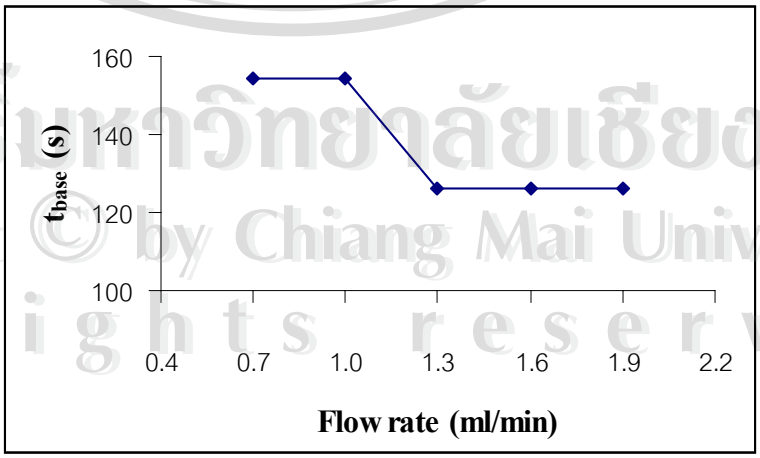

Figure 3.21 Relationship between t_{base} and flow rate of KI solution.

It was found that the highest slope of calibration curve was obtained over the range 1.0 to 1.3 ml/min, but lower sample throughput was obtained at flow rate of 1.0 ml/min. Therefore, the flow rate of 1.3 ml/min was chosen as optimum flow rate for further experiments, with a reasonable sample throughput.

3.2.10 Effect of size of tubing for mixing coil M1

The tube diameter can affect the flow rate and hence affect the sensitivity and sample throughput. Therefore it is important to find out an appropriate inner diameter of mixing tubing. Optimization of inner diameter was studied over the range 0.051 to 0.127 cm. The results in Tables 3.14-3.15 and Figures 3.22-3.24 indicated that the slope of calibration curve increased with the inner diameter (from 0.051 to 0.076 cm) When inner diameter was greater than 0.076 cm, the slope decreased. Therefore the mixing tubing with the inner diameter of 0.076 cm was chosen as optimum with good linearity.

Table 3.14 Effect of size of mixing tubing on peak height.

[Se(IV)] (ppm)	Peak height (mV) obtained for size of mixing tubing (cm i.d.)			
	0.051	0.076	0.102	0.127
0.1	0.60	0.92	0.80	0.52
0.2	1.00	2.08	1.52	1.12
0.3	1.80	3.12	2.52	1.68
0.4	2.32	3.88	3.68	2.00
0.5	2.68	5.08	4.08	2.60
Slope (mV/ppm)	5.53	10.09	8.58	5.14
Correlation coefficient	0.9907	0.9975	0.9894	0.9948

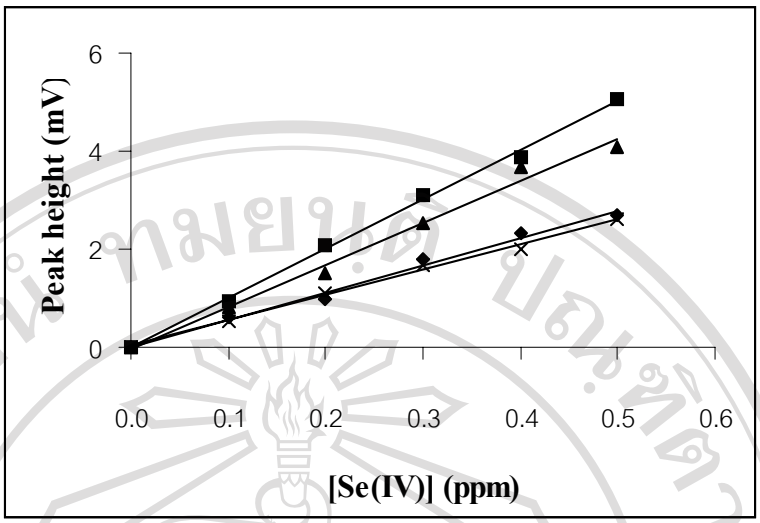

Figure 3.22 Effect of size of mixing tubing on peak height: (a) 0.051; (b) 0.076; (c) 0.102; and (d) 0.127 cm.

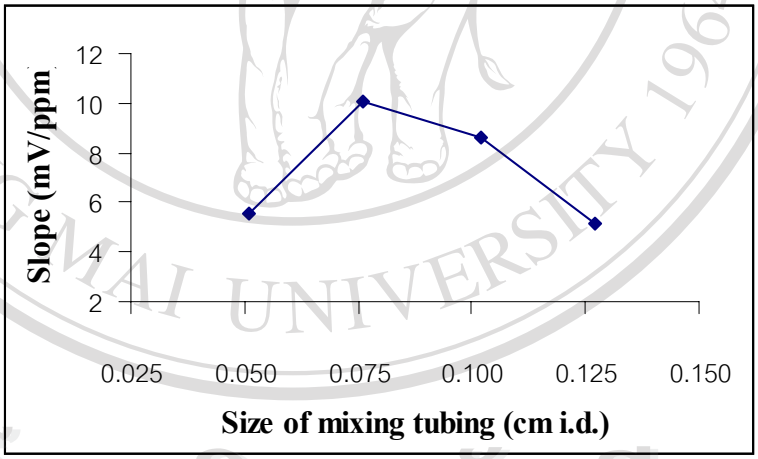

Figure 3.23 Relationship between slope and size of mixing tubing.

Table 3.15 Analytical characteristics at various sizes of mixing tubing.

Size of mixing tubing (cm i.d.)	Peak width (cm)	t_{base} (s)	Sample/h
0.051	0.33	144	25
0.076	0.33	144	25
0.102	0.33	144	25
0.127	0.27	116	31

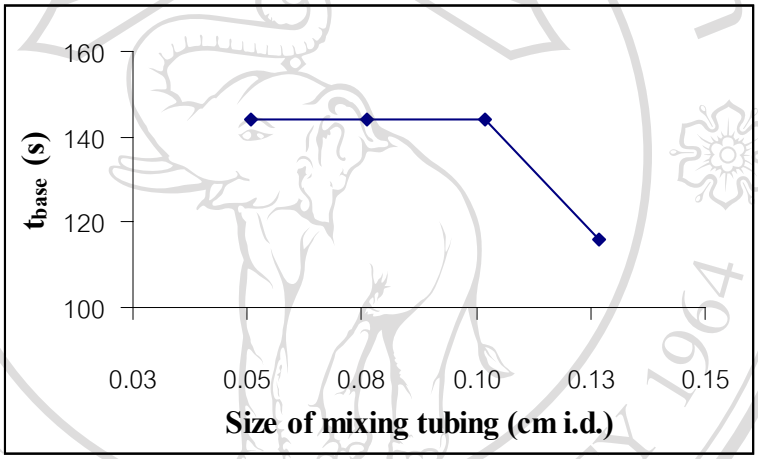

Figure 3.24 Relationship between t_{base} and size of mixing tubing.

3.2.11 Effect of length of tubing for mixing coil M1

The length of mixing tubing can affect the flow rate and thus, the sensitivity and sample throughput. It is necessary to investigate the optimum length to obtain the best sensitivity and adequate sample throughput. Optimization was carried out by varying the length of tygon tubing over the range 50 to 250 cm. The results as shown in Tables 3.16-3.17 and Figures 3.25-3.27 indicated that the slope increased with the length of mixing tubing up to 150 cm. Afterwards, the slope decreased with longer mixing tubing. Therefore the 150 cm was chosen as optimum length for mixing coil M1 due to highest sensitivity and sample throughput

Table 3.16 Effect of length of mixing tubing on peak height.

[Se(IV)] (ppm)	Peak height (mV) obtained for length of mixing tubing (cm)				
	50	100	150	200	250
0.1	0.84	1.00	1.08	1.08	0.88
0.2	1.60	1.92	2.00	2.12	1.80
0.3	2.52	2.88	3.28	2.80	2.40
0.4	3.40	4.08	4.48	4.20	3.28
0.5	4.08	4.92	5.28	4.72	4.32
Slope (mV/ppm)	8.28	9.94	10.82	9.61	8.40
Correlation coefficient	0.9987	0.9985	0.9968	0.9907	0.9960

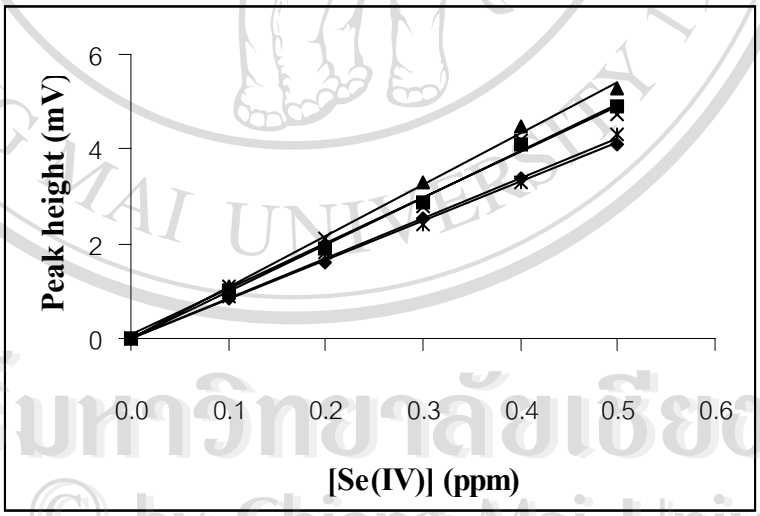

Figure 3.25 Effect of length of mixing tubing on peak height: (a) 50; (b) 100; (c) 150; (d) 200 and (e) 250 cm.

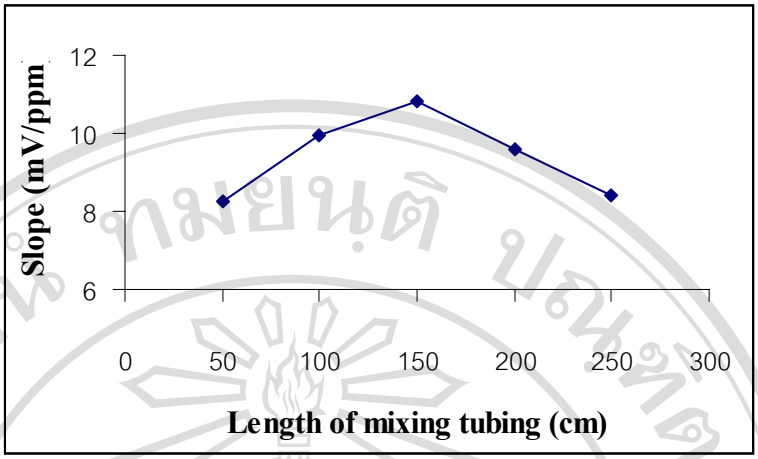

Figure 3.26 Relationship between slope and length of mixing tubing.

Table 3.17 Analytical characteristics at various lengths of mixing tubing.

Length of mixing tubing (cm)	Peak width (cm)	t_{base} (s)	Sample/h
50	0.25	108	33
100	0.25	108	33
150	0.25	108	33
200	0.28	120	30
250	0.28	120	30

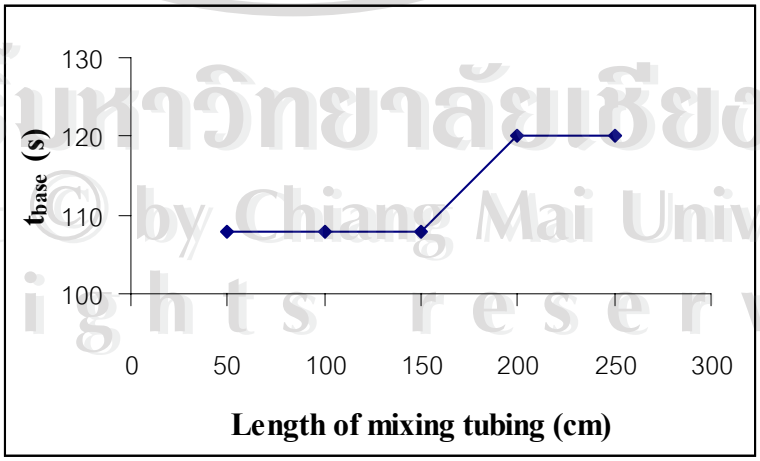

Figure 3.27 Relationship between t_{base} and length of mixing tubing.

3.2.12 Effect of size of test tube for mixing coil M1

The mixing coil was made of narrow-bore tubing by winding round a glass test tube. The size of test tube can affect the sensitivity of measurement. Optimization of the size of test tube was carried out by varying the outer diameter of test tube over the range 1.0 to 2.4 cm.

Table 3.18 Effect of size of test tube on peak height.

[Se(IV)] (ppm)	Peak height (mV) obtained for size of test tube (cm o.d.)			
	1.0	1.5	1.9	2.4
0.1	0.72	1.00	1.08	0.80
0.2	1.60	2.08	2.32	1.72
0.3	2.52	2.60	3.48	2.28
0.4	3.12	4.20	4.20	2.92
0.5	3.88	4.72	5.40	3.48
Slope (mV/ppm)	7.86	9.63	10.72	6.95
Correlation coefficient	0.9969	0.9858	0.9959	0.9909

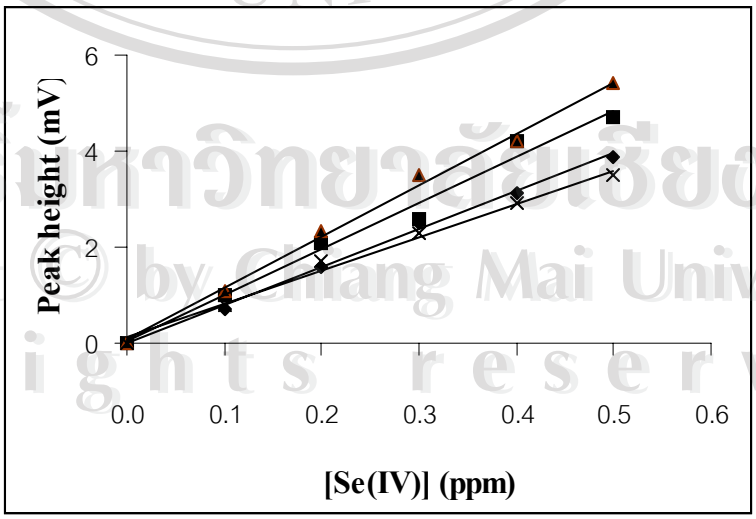

Figure 3.28 Effect of size of test tube on peak height: (a) 1.0; (b) 1.5; (c) 1.9; and (d) 2.4 cm.

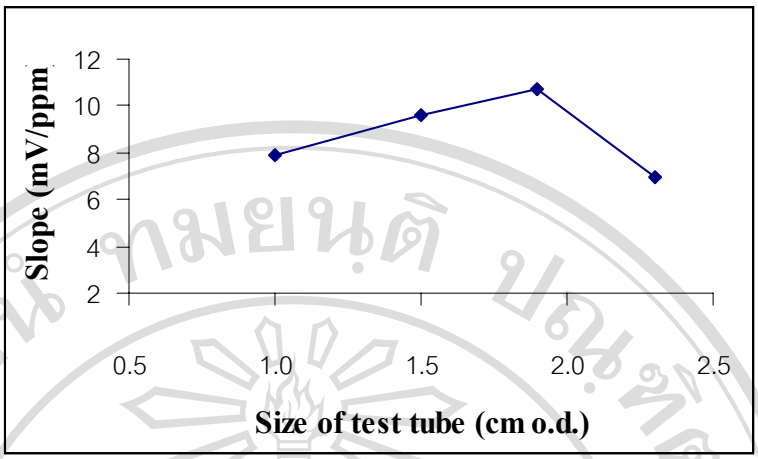

Figure 3.29 Relationship between slope and size of test tube.

Table 3.19 Analytical characteristics at various sizes of test tube.

Size of test tube (cm o.d.)	Peak width (cm)	t_{base} (s)	Sample/h
1.0	0.24	105	34
1.5	0.27	117	31
1.9	0.24	105	34
2.4	0.24	105	34

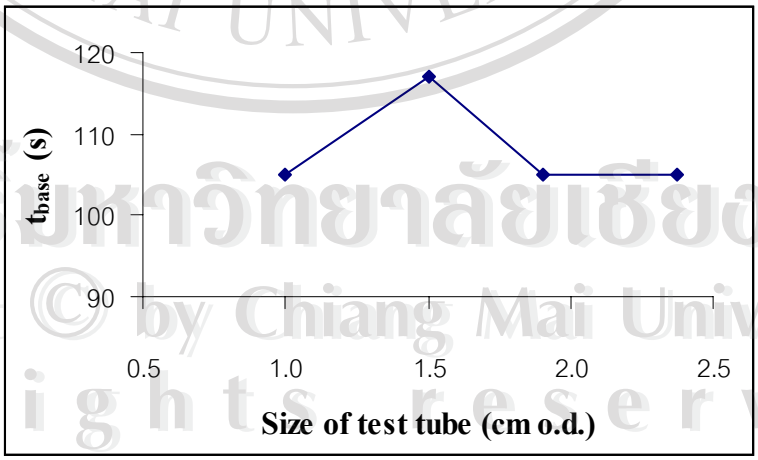

Figure 3.30 Relationship between t_{base} and size of test tube.

The results as shown in Tables 3.18-3.19 and Figures 3.28-3.30 indicated that the sensitivity increased with increasing size of test tube up to 1.9 cm o.d., which was therefore chosen as optimum size of test tube for subsequent studies, with reasonable sample throughput and linearity.

3.2.13 Effect of type of mixing part M1

The function of mixing reactor is to increase the degree of mixing. The coiled tube has been the most frequent geometric form of the FIA microreactor. However, it is useful to review channel geometries. The influence of various types of mixing reactors on the dispersion were studied to achieve homogeneous mixing of sample and HCl streams. The types of mixing parts namely coil, straight, knitted and zig zag (2×2 cm) were tested. Tables 3.20-3.21 and Figures 3.31-3.33 showed that the high sensitivity was obtained with knitted and zig zag reactors, but correlation coefficient obtained by using knitted reactor is better than that obtaing by using zig zag reactor. This indicated that knitted reactor was suitable because it was sufficient to promote the mixing in the flow channel.

Table 3.20 Effect of type of mixing part on peak height.

[Se(IV)] (ppm)	Peak height (mV) obtained for type of mixing part			
	straight	coiled	knitted	zig zag
0.1	1.28	1.08	2.48	2.24
0.2	2.40	2.12	5.32	4.60
0.3	3.48	3.00	7.68	6.48
0.4	5.12	4.52	9.52	9.12
0.5	6.68	5.08	12.92	10.80
Slope (mV/ppm)	13.14	10.46	25.17	21.86
Correlation coefficient	0.9933	0.9920	0.9954	0.9978

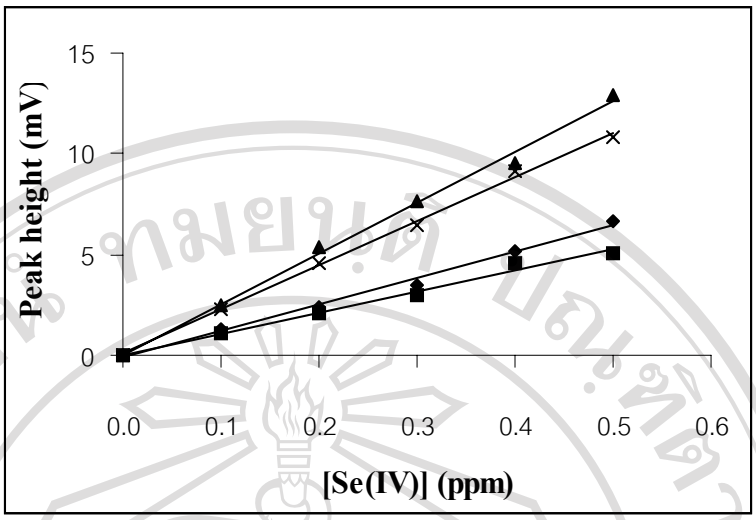

Figure 3.31 Effect of type of mixing part on peak height: (a) straight; (b) coiled; (c) knitted; and (d) zig zag reactor.

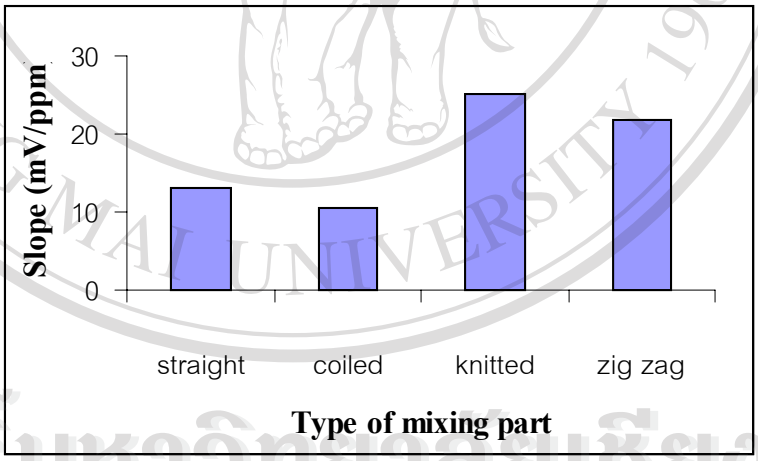

Figure 3.32 Relationship between slope and type of mixing part.

Table 3.21 Analytical characteristics at various types of mixing parts.

Type of mixing part	Peak width (cm)	t_{base} (s)	Sample/h
Straight	0.23	100	36
Coiled	0.25	108	33
Knitted	0.25	108	33
Zig zag	0.25	108	33

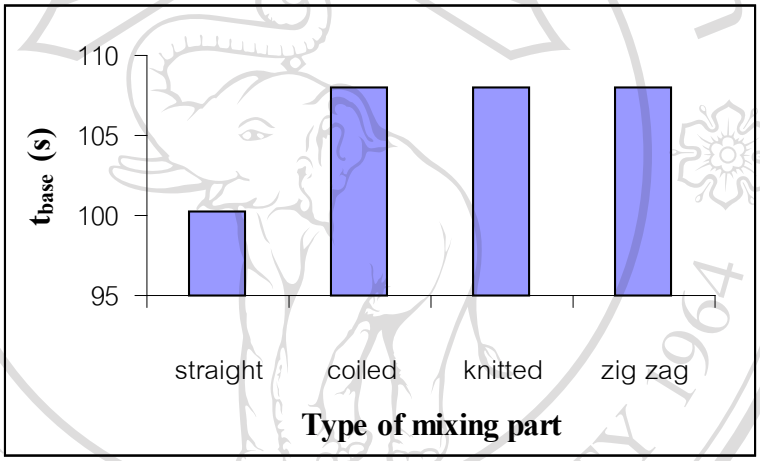

Figure 3.33 Relationship between t_{base} and type of mixing part.

3.2.14 Effect of size of tubing for mixing coil M2

The effect of inner diameter of tubing for mixing coil M2 was studied by varying the inner diameter of mixing tubing in the range of 0.051 to 0.132 cm. The results obtained showed that the sensitivity increased with the inner diameter up to 0.107 cm. Afterwards, the sensitivity decreased until inner diameter was 0.132 cm. The sample throughput was stable (from 0.051 to 0.132 cm). Therefore an inner diameter of 0.107 cm was selected as optimum inner diameter of mixing tubing for mixing coil M2.

Table 3.22 Effect of size of mixing tubing on peak height

[Se(IV)] (ppm)	Peak height (mV) obtained for size of mixing tubing (cm i.d.)			
	0.051	0.086	0.107	0.132
0.1	1.80	2.20	2.48	1.20
0.2	3.68	4.80	5.60	3.52
0.3	5.28	6.92	7.40	5.92
0.4	7.28	8.48	9.68	7.40
0.5	8.72	10.32	13.32	10.28
Slope (mV/ppm)	17.61	20.73	25.71	20.69
Correlation coefficient	0.9987	0.9930	0.9923	0.9899

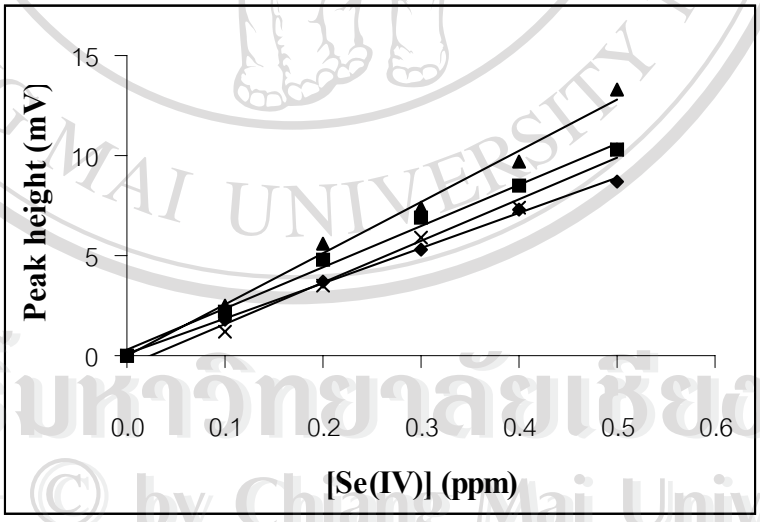

Figure 3.34 Effect of size of mixing tubing on peak height: (a) 0.051; (b) 0.086; (c) 0.107; and (d) 0.132 cm.

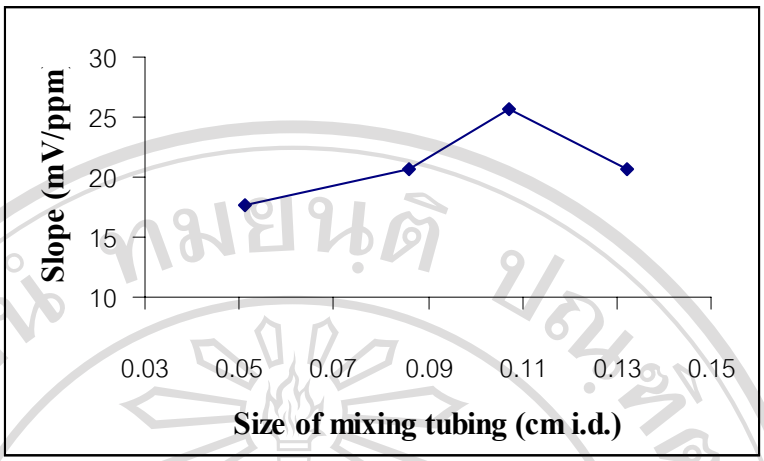

Figure 3.35 Relationship between slope and size of mixing tubing.

Table 3.23 Analytical characteristics at various sizes of mixing tubing.

Size of mixing tubing (cm i.d.)	Peak width (cm)	t_{base} (s)	Sample/h
0.051	0.24	103	35
0.086	0.24	103	35
0.107	0.24	103	35
0.132	0.24	103	35

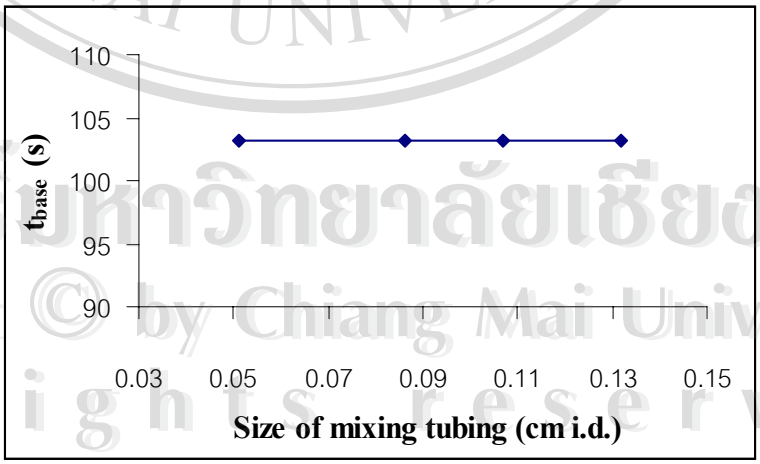

Figure 3.36 Relationship between t_{base} and size of mixing tubing.

3.2.15 Effect of length of tubing for mixing coil M2

The dispersion in FIA system caused by the flow in the narrow tube depend on the distance traveled of the sample zone. The influence of the length of mixing tubing for mixing coil M2 on dispersion was investigated in order to obtain maximum sensitivity and thus sample throughput by varying the length from 50 to 250 cm. The results in Tables 3.24-3.25 and Figures 3.37-3.39 showed that the slope increased when the length decreased (from 100 to 250 cm). As regards to sensitivity, a 100 cm tube length was therefore chosen as optimum condition for subsequent experiments because it provided highest sensitivity and appropriate sample throughput which is the essence of using FI method. The length of mixing tubing is defined as the portion or part of tubing, where the sample and reagent are mixed and reacted which means that this optimum length allowed sufficient time available for the oxidation reaction between iodide and selenite as mentioned to proceed efficiently.

Table 3.24 Effect of length of mixing tubing on peak height.

[Se(IV)] (ppm)	Peak height (mV) obtained for length of mixing tubing (cm)				
	50	100	150	200	250
0.1	2.08	2.40	1.60	1.80	1.20
0.2	4.20	5.00	3.52	2.88	2.52
0.3	6.40	7.72	5.28	4.32	3.92
0.4	8.08	9.32	6.28	6.12	4.88
0.5	10.4	12.72	8.32	8.20	5.68
Slope (mV/ppm)	20.63	24.88	16.40	15.83	11.67
Correlation coefficient	0.9989	0.9950	0.9946	0.9908	0.9917

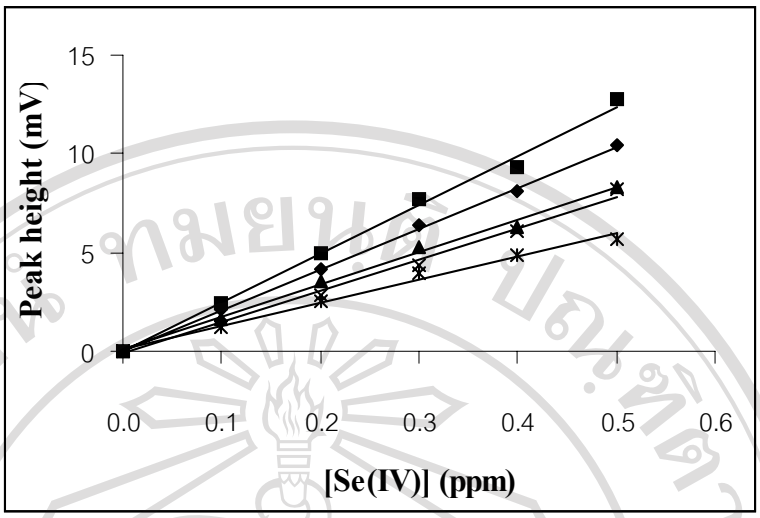

Figure 3.37 Effect of length of mixing tubing on peak height: (a) 50; (b) 100; (c) 150; (d) 200; and (e) 250 cm.

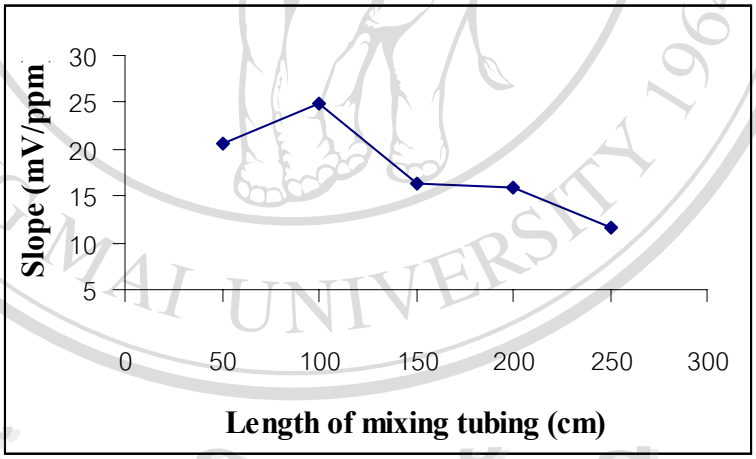

Figure 3.38 Relationship between slope and length of mixing tubing.

Table 3.25 Analytical characteristics at various lengths of mixing tubing.

Length of mixing tubing (cm)	Peak width (cm)	t_{base} (s)	Sample/h
50	0.22	94	38
100	0.22	94	38
150	0.22	97	37
200	0.22	97	37
250	0.22	97	37

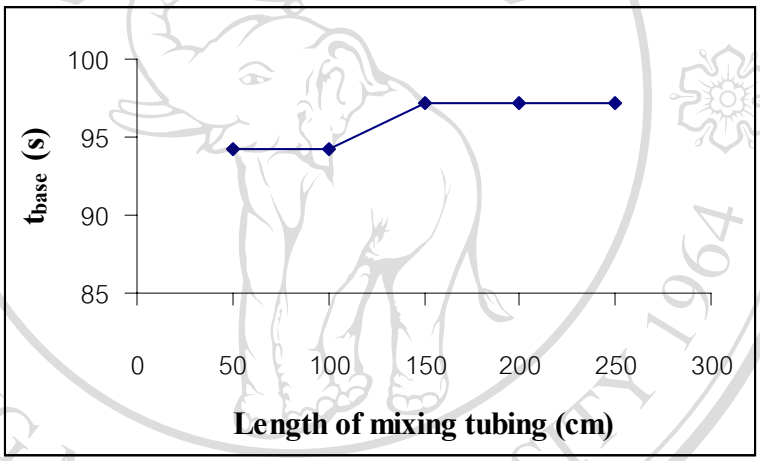

Figure 3.39 Relationship between t_{base} and length of mixing tubing.

3.2.16 Effect of size of test tube for mixing coil M2

The effect of size of test tube for mixing coil M2 on degree of mixing between iodide and selenite in acidic medium in oxidation reaction was investigated by varying the outer diameter of test tube from 1.0 to 2.4 cm. The results obtained were shown in Tables 3.26-3.27 and Figures 3.40-3.42. It can be seen that the optimum size of test tube for this mixing coil was 1.9 cm because it provided more satisfactory sensitivity and sample throughput.

Table 3.26 Effect of size of test tube on peak height.

[Se(IV)] (ppm)	Peak height (mV) obtained for size of test tube (cm o.d.)			
	1.0	1.5	1.9	2.4
0.1	1.72	2.20	2.40	1.60
0.2	3.28	4.08	4.88	3.48
0.3	4.52	6.00	7.92	4.80
0.4	6.92	9.08	10.12	6.40
0.5	8.20	10.12	12.40	7.52
Slope (mV/ppm)	16.53	20.93	25.20	15.23
Correlation coefficient	0.9939	0.9907	0.9981	0.9951

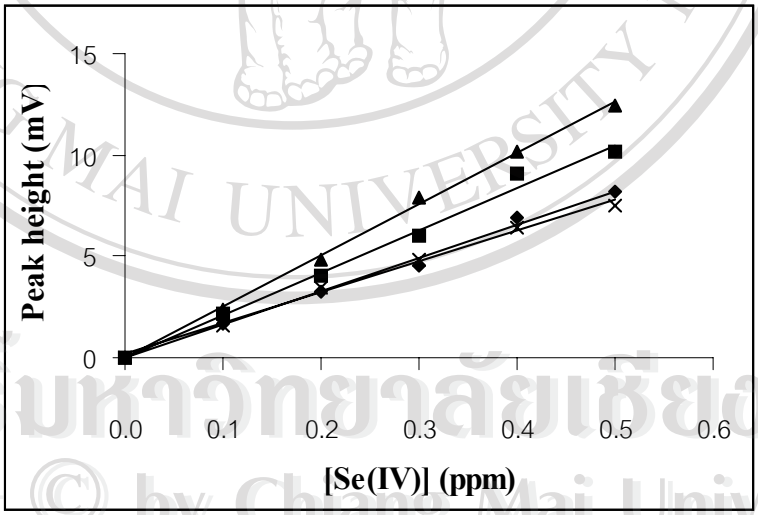

Figure 3.40 Effect of size of test tube on peak height: (a) 1.0; (b) 1.5; (c) 1.9; and (d) 2.4 cm.

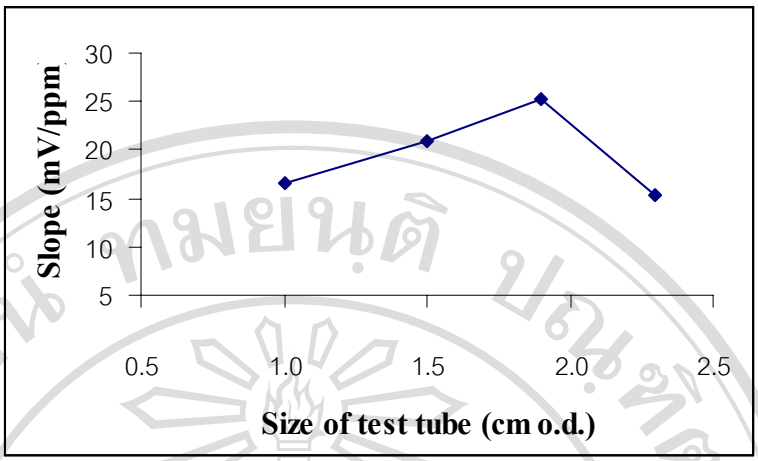

Figure 3.41 Relationship between slope and size of test tube.

Table 3.27 Analytical characteristics at various sizes of test tube.

Size of test tube (cm o.d.)	Peak width (cm)	t_{base} (s)	Sample/h
1.0	0.21	92	39
1.5	0.21	92	39
1.9	0.21	90	40
2.4	0.21	92	39

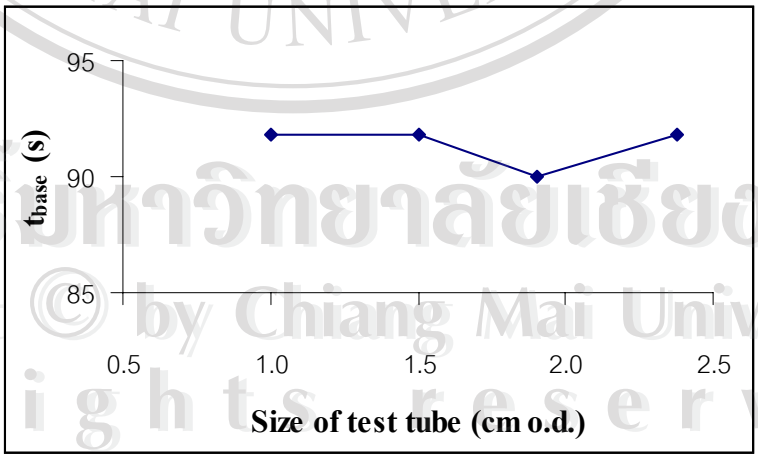

Figure 3.42 Relationship between t_{base} and size of test tube.

3.2.17 Effect of size of mixing tubing for mixing coil M3

The effect of inner diameter of mixing tubing for mixing coil M3 was investigated in the range of 0.051 to 0.132 cm. The results obtained were shown in Tables 3.28-3.29 and Figures 3.43-3.45.

Table 3.28 Effect of size of mixing tubing on peak height.

[Se(IV)] (ppm)	Peak height (mV) obtained for size of mixing tubing (cm i.d.)			
	0.051	0.086	0.107	0.132
0.1	2.60	2.40	2.48	3.28
0.2	5.72	4.88	5.68	7.00
0.3	8.52	6.52	7.48	9.72
0.4	9.52	9.00	10.52	14.52
0.5	12.48	12.20	13.12	16.20
Slope (mV/ppm)	24.56	23.55	26.15	33.55
Correlation coefficient	0.9863	0.9932	0.9970	0.9913

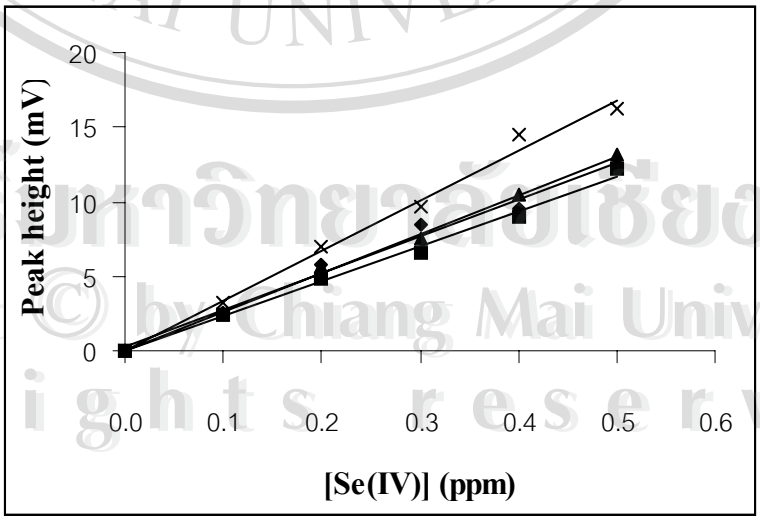

Figure 3.43 Effect of size of mixing tubing on peak height: (a) 0.051; (b) 0.086; (c) 0.107; and (d) 0.132 cm.

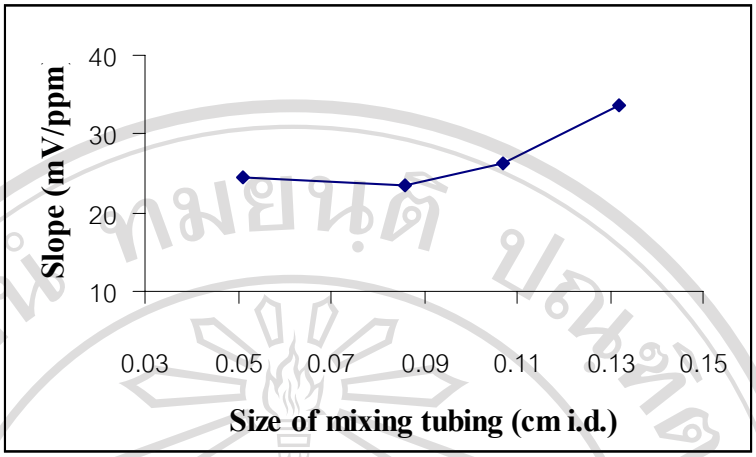

Figure 3.44 Relationship between slope and size of mixing tubing.

Table 3.29 Analytical characteristics at various sizes of mixing tubing.

Size of mixing tubing (cm i.d.)	Peak width (cm)	t_{base} (s)	Sample/h
0.051	0.21	91	40
0.086	0.21	91	40
0.107	0.19	80	45
0.132	0.21	91	40

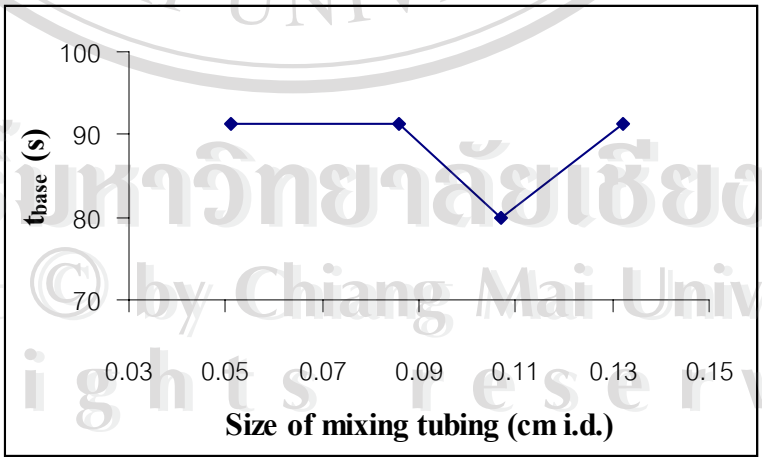

Figure 3.45 Relationship between t_{base} and size of mixing tubing.

It was found that the slope of calibration curve was quite stable with increasing inner diameter up to 0.107 cm. The highest slope was obtained when the inner diameter was 0.132 cm. Therefore, the 0.132 cm inside diameter of mixing tubing was chosen for further measurements as a compromise between sensitivity and sample throughput, with reasonable linearity.

3.2.18 Effect of length of tubing for mixing coil M3

It is necessary to optimize the tube length to obtain sufficient time for color development in complexation reaction. The effect of tube length for mixing coil M3 on peak height was investigated over the range 50 to 250 cm. The results obtained are exhibited in Tables 3.30-3.31 and Figures 3.46-3.48. It can be seen that the greater slope of calibration curve were obtained when the length of the mixing tubing decreased. Therefore the 100 cm length of mixing tubing was chosen for further experiment because it provided best sensitivity with good linearity of the calibration curve and reasonable sampling rate.

Table 3.30 Effect of length of mixing tubing on peak height.

[Se(IV)] (ppm)	Peak height (mV) obtained for length of mixing tubing (cm)				
	50	100	150	200	250
0.1	2.36	3.12	2.08	1.32	0.76
0.2	4.92	6.48	3.40	2.12	1.80
0.3	6.60	9.40	5.68	3.96	2.48
0.4	8.68	13.00	7.12	4.92	3.12
0.5	11.80	17.08	8.12	6.60	3.68
Slope (mV/ppm)	22.75	33.70	16.57	13.04	7.47
Correlation coefficient	0.9940	0.9972	0.9885	0.9911	0.9895

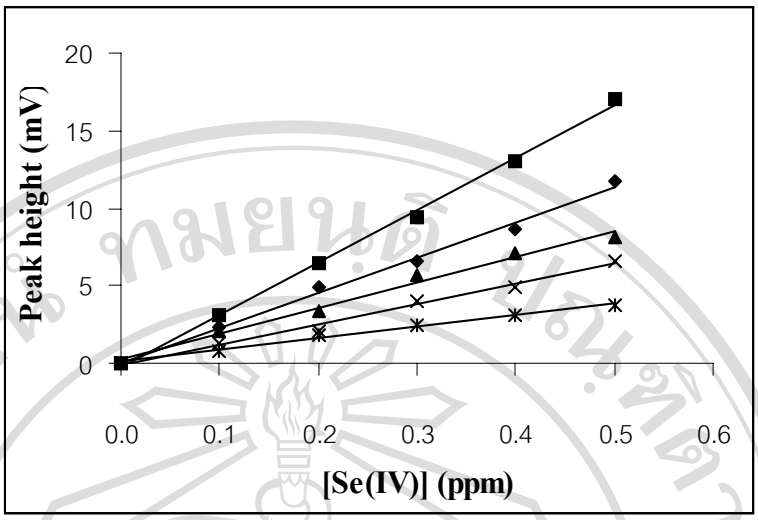

Figure 3.46 Effect of length of mixing tubing on peak height: (a) 50; (b) 100; (c) 150; (d) 200; and (e) 250 cm.

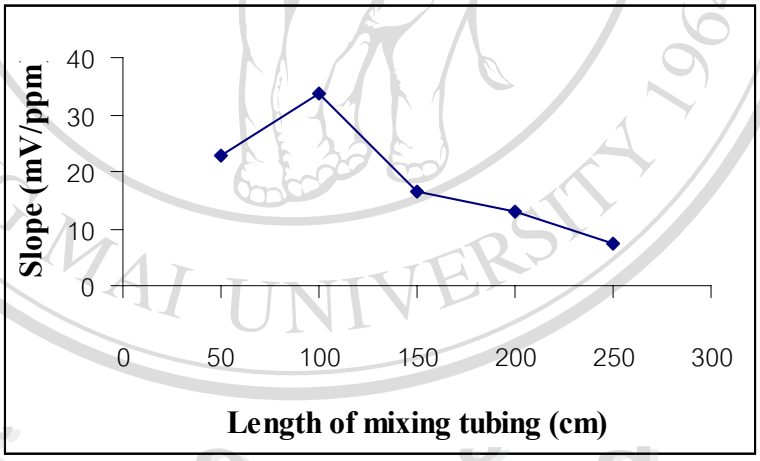

Figure 3.47 Relationship between slope and length of mixing tubing.

Table 3.31 Analytical characteristics at various lengths of mixing tubing.

Length of mixing tubing (cm)	Peak width (cm)	t_{base} (s)	Sample/h
50	0.15	65	55
100	0.15	65	55
150	0.18	76	47
200	0.18	76	47
250	0.18	76	47

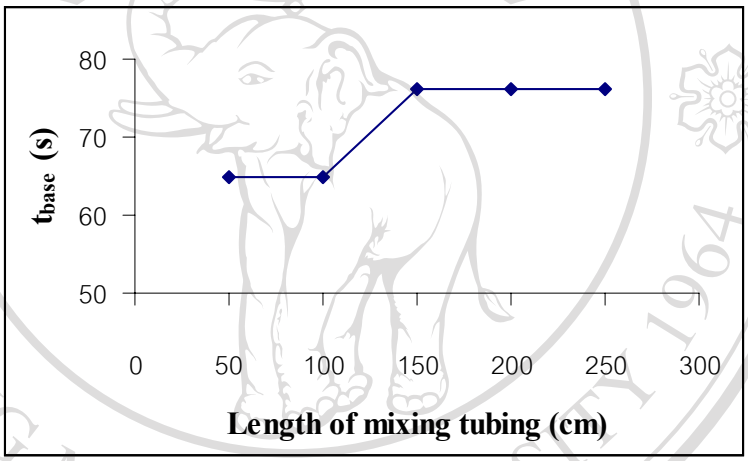

Figure 3.48 Relationship between t_{base} and length of mixing tubing.

3.2.19 Effect of size of test tube for mixing coil M3

The channel geometry of reactor affects the dispersion in real flow system, so it is necessary to investigate the optimum size of test tube for mixing coil in order to obtain the maximum sensitivity. The effect of various sizes of test tube for mixing coil M3 (1.0 to 2.4 cm o.d.) on peak height was studied as can be seen in Tables 3.32-3.33 and Figures 3.49-3.51. The results indicated that the largest slope with better linearity of standard calibration curve was obtained when the size of test tube was 1.9 cm.

Table 3.32 Effect of size of test tube on peak height.

[Se(IV)] (ppm)	Peak height (mV) obtained for size of test tube (cm o.d.)			
	1.0	1.5	1.9	2.4
0.1	1.12	1.52	3.24	3.28
0.2	2.24	3.04	7.28	6.00
0.3	3.52	5.00	10.52	10.92
0.4	4.48	6.08	12.08	14.00
0.5	5.28	8.52	16.80	14.92
Slope (mV/ppm)	10.79	16.64	32.50	31.91
Correlation coefficient	0.9954	0.9924	0.9887	0.9764

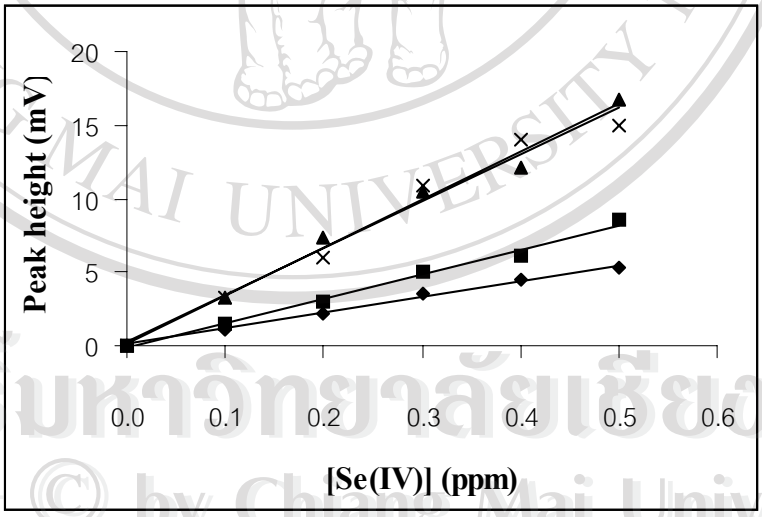

Figure 3.49 Effect of size of test tube on peak height: (a) 1.0; (b) 1.5; (c) 1.9; and (d) 2.4 cm.

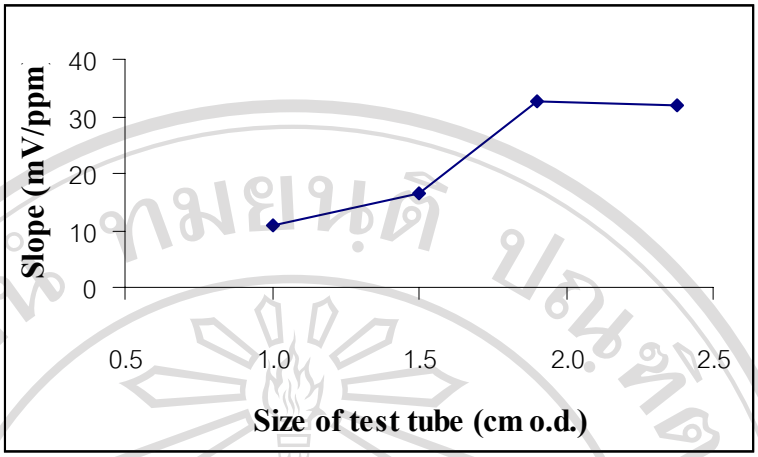

Figure 3.50 Relationship between slope and size of test tube.

Table 3.33 Analytical characteristics at various sizes of test tube.

Size of test tube (cm o.d.)	Peak width (cm)	t_{base} (s)	Sample/h
1.0	0.14	62	58
1.5	0.14	62	58
1.9	0.14	62	58
2.4	0.14	62	58

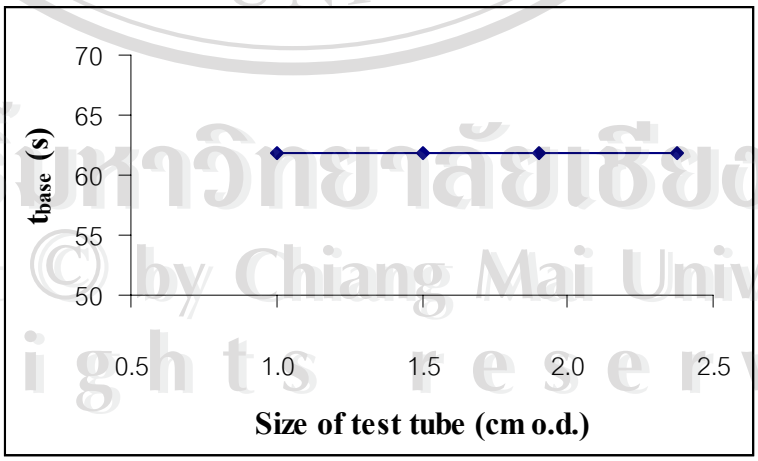

Figure 3.51 Relationship between t_{base} and size of test tube

3.2.20 Effect of Injection volume

The injection volume of complexing agent, rhodamine B, is one of significant flow parameters. The dispersion in FIA system depend on injection volume. Therefore changing the injected reagent volume is a powerful way to change dispersion. The injection volume was optimized in order to obtained adequate sensitivity and thus, sample throughput. This effect was investigated by varying the loop length of injection valve to give an injection volume over the range 150 to 350 µl. The resulting experimental observations were shown in Tables 3.34-3.35 and Figures 3.52-3.54. It was found that by injecting increasing volume of dye solution, the sensitivity increased until the injection volume increased up to 250 µl. The highest slope was obtained in the range of 250 to 350 µl, but the better linearity of calibration curve was obtained when the injection volume was 250 µl. The sample throughput were stable with injection volume. Therefore, an injection volume of 250 µl was found to be the optimum condition with low reagent consumption and highest sensitivity.

Table 3.34 Effect of injection volume on peak height.

[Se(IV)] (ppm)	Peak height (mV) obtained for injection volume (µl)				
	150	200	250	300	350
0.1	3.24	4.12	4.92	5.92	6.20
0.2	6.88	8.24	11.80	11.52	9.12
0.3	9.08	13.12	15.40	14.28	17.40
0.4	13.68	17.68	19.92	23.68	21.08
0.5	16.20	20.08	27.28	26.12	25.32
Slope (mV/ppm)	32.72	41.70	52.86	53.33	51.29
Correlation coefficient	0.9945	0.9938	0.9917	0.9814	0.9869

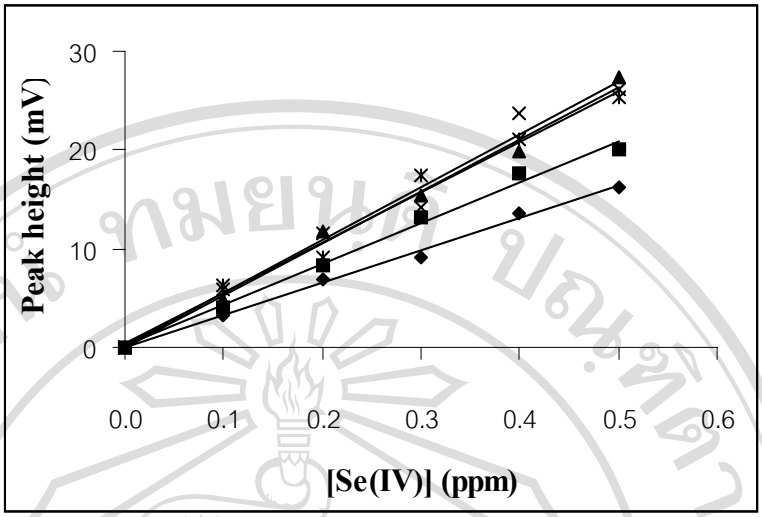

Figure 3.52 Effect of injection volume on peak height: (a) 150; (b) 200; (c) 250; (d) 300; and (e) 350 µl.

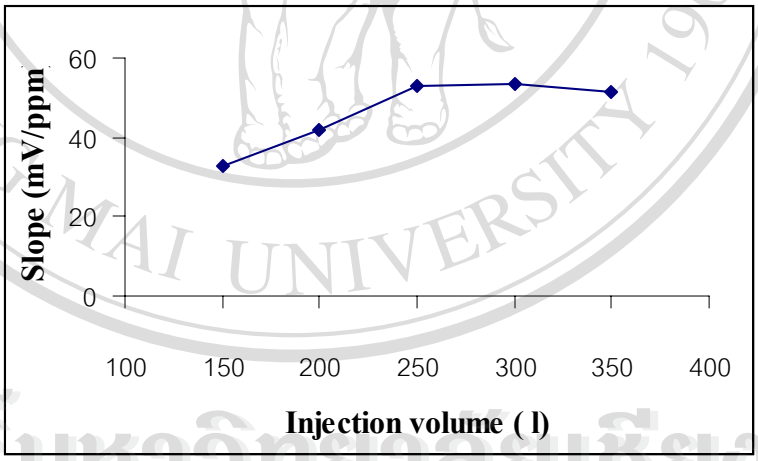

Figure 3.53 Relationship between slope and injection volume.

Table 3.35 Analytical characteristics at various injection volumes.

Injection volume (µl)	Peak width (cm)	t_{base} (s)	Sample/h
150	0.10	43	84
200	0.10	43	84
250	0.10	43	84
300	0.10	43	84
350	0.12	53	68

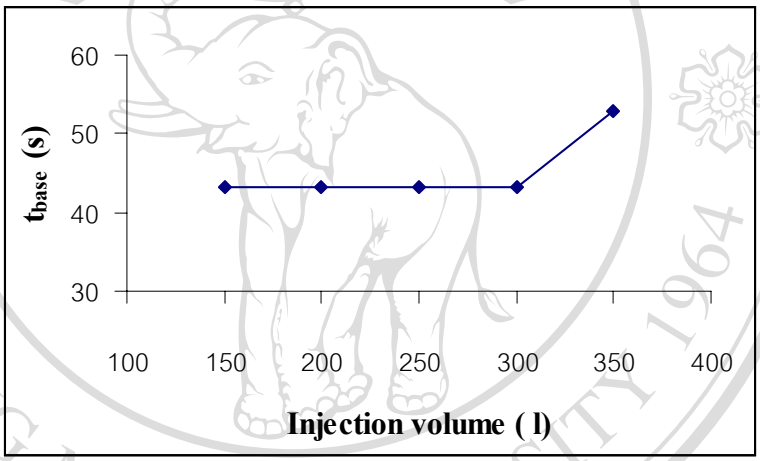

Figure 3.54 Relationship between t_{base} and Injection volume.

3.2.21 Effect of irradiation time

A procedure for the on-line prereduction and determination of selenite and selenate was carried out by incorporation of UV lamp into flow system. The reduction of selenate (non-complex forming) to selenite (complex forming) is influenced by irradiation time. To reduce selenate quantitatively to selenite, the reduction was investigated by varying irradiation times ranging from 0 to 210 s. The results in Table 3.36 and Figure 3.55 indicated that without irradiation the signal is not obtained , which means that the reduction did not take place, and after irradiation of 120 s, there was a decrease in the peak-height signal. This might have been due to photooxidation of selenite to

selenate, thus irradiation time of 120 s were adoped, as it allowed the highest efficiency of reduction.

Table 3.36 Effect of irradiation time on peak height.

Irradiation time (s)	Peak height	
	cm	mV
0	0	0
30	0.47	1.88
60	0.65	2.60
90	0.75	3.00
120	0.80	3.20
150	0.74	2.96
180	0.72	2.88
210	0.71	1.84

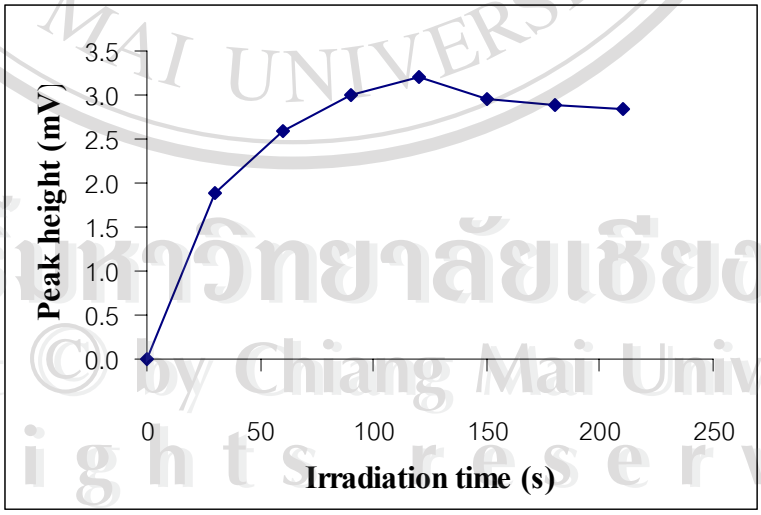

Figure 3.55 Effect of irradiation time on peak height.

3.3 Study of the analytical characteristics

Obtained experimental parameters for selenium speciation are summarized in Table 3.37. These optimum conditions were used for further work.

Table 3.37 Experimental conditions for selenium determination.

Condition	Information
HCl concentration (M)	0.25
KI concentration (M)	0.23
NaOAc concentration (M)	0.10
PVA concentration (% w/v)	1.0
RhB concentration (M)	2.0×10^{-4}
Flow rate of sample solution (ml/min)	1.0
Flow rate of HCl solution (ml/min)	1.0
Flow rate of KI solution (ml/min)	1.3
Type of mixing part M1	knitted
Size of mixing tubing for mixing part M1 (cm i.d.)	0.076
Length of mixing tubing for mixing part M1 (cm)	150
Size of mixing tubing for mixing coil M2 (cm i.d.)	0.107
Length of mixing tubing for mixing coil M2 (cm)	100
Size of test tube for mixing coil M2 (cm o.d.)	1.9
Size of mixing tubing for mixing coil M3 (cm i.d.)	0.132
Length of mixing tubing for mixing coil M3 (cm)	100
Size of test tube for mixing coil M3 (cm o.d.)	1.9
Injection volume (μl)	250
Irradiation time (s)	120
Chart speed (cm/h)	10
Sensitivity (mV/cm)	4

3.3.1 Linearity

The linear range of the proposed method for determination of selenite and selenate was studied by introducing various selenite and selenate standard slolutions (0.0-4.0 ppm) into the flow system under the suitable conditions as shown in Table 3.37. The results obtained are presented in Table 3.38 and Figures 3.56-3.57. The experimental results indicated that linear range was in the range of 0.0-1.0 ppm for selenite and selenate, which means that beer's law was obeyed over a wide concentration range, which is useful for analysis of both species in diverse matrices of samples.

Table 3.38 Study of linear range.

[Se] (ppm)	Peak height (mV)	
	Selenite	Selenate
0.0	0.00	0.00
0.1	4.00	1.56
0.2	7.88	2.72
0.3	11.84	3.88
0.4	15.76	5.00
0.5	19.68	6.16
0.6	23.60	7.28
0.8	31.52	9.6
1.0	36.80	11.88
1.5	51.68	16.68
2.0	62.24	20.08
3.0	72.64	23.44
4.0	75.12	25.08

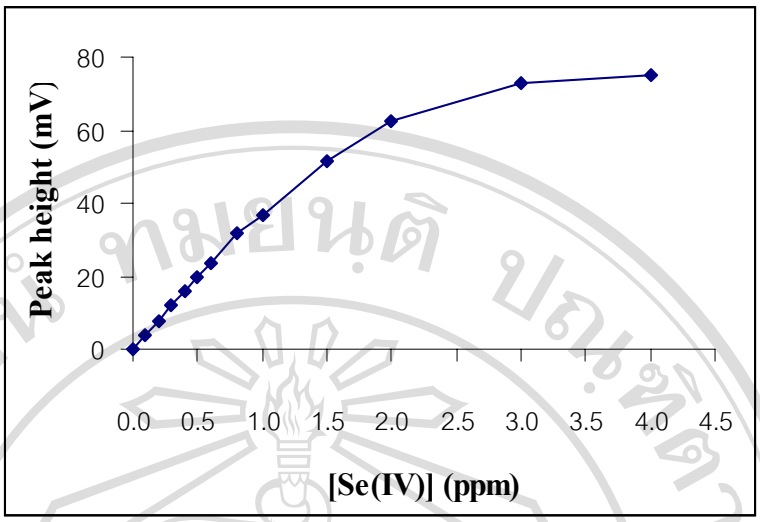

Figure 3.56 Relationship between peak height and various concentrations of selenite.

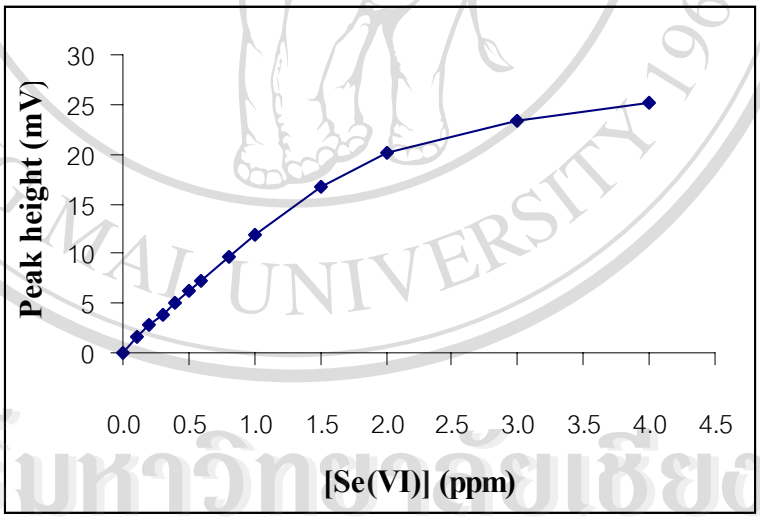

Figure 3.57 Relationship between peak height and various concentrations of selenate.

3.3.2 Precision

1) Precision of the flow injection system

The precision of the flow injection system was determined by repeating 10 injections of complexing agent for 0.2 ppm selenite and selenate standard solutions into the proposed FI system. The results obtained are shown in Table 3.39. The results exhibited that the precision with replicate injections, expressed as the relative standard deviation (RSD), were found to be 1.21% and 2.37% for selenite and selenate. The experimental results indicated that the proposed flow system provided good repeatability (less than 5% RSD) for two these species under the optimum conditions.

Table 3.39 Study of precision of the flow injection system.

Expt. no.	Peak height (mV)	
	Selenite	Selenate
1	7.80	2.80
2	7.80	2.80
3	7.80	2.80
4	7.80	2.80
5	7.60	2.80
6	7.80	2.80
7	7.80	2.80
8	7.80	3.00
9	8.00	2.80
10	7.80	2.80
Mean	7.80	2.80
SD	0.0940	0.0664
%RSD	1.21	2.37

2) Precision of the proposed FI method

The precision of the proposed FI method was determined by preparing ten standard solutions containing 0.2 ppm selenite and selenate, which were then introduced into the proposed FI system under the experimental conditions. The RSD for replicate determinations were found to be 1.83% and 4.43% for selenite and selenate as shown in Table 3.40. These experimental results indicated that the proposed method was reproducible. The statistical formulae used in assessing the quality of quantitative data are given in Appendix B.

Table 3.40 Study of precision of the proposed FI method.

Expt. no.	Peak height (mV)	
	Selenite	Selenate
1	7.20	2.60
2	7.20	2.60
3	7.00	2.60
4	7.20	2.40
5	7.40	3.60
6	7.20	2.80
7	7.00	2.60
8	7.40	2.60
9	7.20	2.80
10	7.20	2.60
Mean	7.20	2.60
SD	0.133	0.115
%RSD	1.83	4.43

3.3.3 Detection limit

For investigation of detection limit, the detection limit of the proposed method was investigated by preparing various standard solutions containing low concentrations of selenite and selenate which were introduced into the proposed FI system. The results are given in Tables 3.41 and 3.42. The detection limits (defined as the concentration of the analyte which give the signal equivalent to three times of the standard deviation of the blank signal) were found to be 0.005 ppm and 0.01 ppm for selenite and selenate. The method was found to be sensitive as little as ppb level for selenium could be determined, which allow the detection of selenium in environmental water samples where selenium concentrations were mostly in ppb range.

Table 3.41 Peak height obtained for blank solution.

Expt. no.	Peak height (mV)	
	Selenite	Selenate
1	3.60	0.80
2	3.60	0.80
3	3.60	0.80
4	3.60	0.80
5	3.60	0.72
6	3.40	0.80
7	3.60	0.80
8	3.60	0.80
9	3.80	0.80
10	3.60	0.80
Mean	3.60	0.80
SD	0.0940	0.0668
%RSD	2.67	3.33

Table 3.42 Peak height obtained for low selenite and selenate concentrations.

[Se] (ppm)	Peak height (mV)	
	Selenite	Selenate
0.005	3.84	-
0.010	4.24	1.00
0.030	5.00	1.32
0.050	5.52	1.52
0.070	6.48	1.80

3.3.4 Calibration curve

Linear calibration curves over the concentration range 0.0-0.5 ppm for the determination of selenite and selenate were constructed by introducing standard solutions containing 0.0-0.5 ppm selenite and selenate into the FI system under the optimum conditions (Table 3.37). The results are shown in Table 3.43. The calibration signal was illustrated in Figures 3.58-3.59 and linear calibration curve of each species were plotted in Figures 3.60 to 3.61.

Table 3.43 Peak height for calibration curve.

[Se] (ppm)	Peak height (mV)	
	Selenite	Selenate
0.1	4.08	1.28
0.2	7.68	2.56
0.3	11.32	4.12
0.4	14.92	5.08
0.5	18.56	6.20

Figure 3.58 Calibration signal for determination of selenite.

Figure 3.59 Calibration signal for determination of selenate.

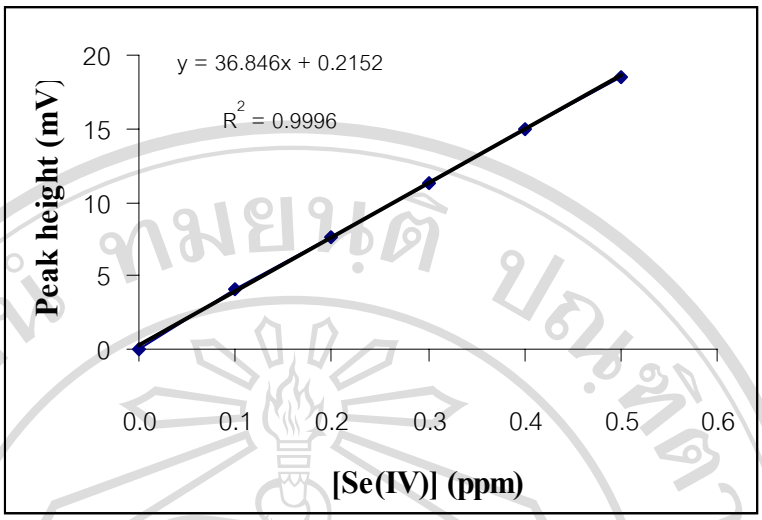

Figure 3.60 The calibration curve of selenite determination.

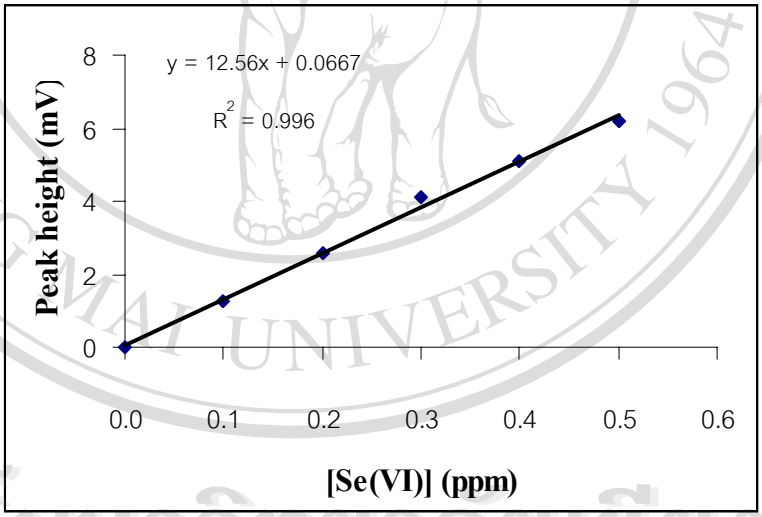

Figure 3.61 The calibration curve of selenate determination.

The calibration curves as shown in Figures 3.58-3.59 were established by plotting peak height against various concentrations of selenite and selenate. Correlation coefficient (r^2) which enables the degree of linearity or correlation to be assess quantitatively and the regression equations are:

$$Y = 36.846X + 0.2152, \ r^2 = 0.9996 \text{ for selenite}$$
$$Y = 12.560X + 0.0667, \ r^2 = 0.9960 \text{ for selenate}$$

Where Y is signal as peak height in mV

X is concentration of selenium concentration in ppm

The values of r^2 obtained indicated good linear relation between analyte concentration and corresponding peak height signal. The sensitivity defined as slope the regression line for selenite and selenate were 36.846 and 12.560 mV/ppm, respectively.

As can be seen in figure 3.61 a straight line which did not passed through all points may be due to indeterminate errors associated with the measurement process.

3.3.5 Accuracy

The accuracy (defined as percentage recovery of the added analyte) of the proposed method was verified by standard addition method. The method was examined by determining the recoveries of the added selenite and selenate with varying concentrations in sample solution. The results are presented in Tables 3.44 and 3.45. The average recoveries were found to be 100.1% and 98.06% for selenite and selenate respectively. The proposed method for determination of two species was found to be accurate for the determination of trace amounts of selenium in sample solutions.

Table 3.44 Peak height obtained by using standard addition method for Se(IV).

[Se(IV)] (ppm)	Peak height (mV)		[Se(IV)] (ppm) found	%recovery
	Std.	Std.+sample		
0.00	-	-	-	-
0.10	4.08	3.80	0.0973	97.3
0.20	7.68	7.92	0.209	105
0.30	11.32	10.92	0.290	96.7
0.40	14.92	15.40	0.412	103
0.50	18.56	18.36	0.492	98.5
Mean			100.1	
SD			3.69	
%RSD			3.68	

Table 3.45 Peak height obtained by using standard addition method for Se(VI).

[Se(VI)] (ppm)	Peak height (mV)		[Se(VI)] (ppm) found	% recovery
	Std.	Std.+sample		
0.00	-	-	-	-
0.10	1.28	1.32	0.0998	99.8
0.20	2.56	2.48	0.192	96.0
0.30	4.12	4.12	0.300	100
0.40	5.08	4.72	0.370	92.5
0.50	6.20	6.48	0.511	102
Mean			98.06	
SD			3.79	
%RSD			3.86	

3.3.6 Interferences

In order to investigate the effect of chemical interferences, some possible interfering ions which generally present in water samples including sodium, potassium, magnesium, calcium, iron, zinc, copper, cadmium, chloride, nitrate, sulphate, carbonate and phosphate was studied before quantitative analysis of sample solutions is carried out. The results are presented in Tables 3.46 and 3.47.

Table 3.46 Effect of interfering ions on selenite determination.

Ion	Se(IV) : Ion	Peak height (mV)	%Relative error
Na^+	1 : 0	7.68	0
	1 : 2	7.68	0
	1 : 5	7.68	0
	1 :10	7.80	1.56
	1 : 20	7.84	2.08
	1 : 50	7.88	2.60
K^+	1 : 0	7.68	0
	1 : 2	7.68	0
	1 : 5	7.68	0
	1 :10	7.68	0
	1 : 20	7.88	2.60
	1 : 50	7.92	3.12
Mg^{2+}	1 : 0	7.68	0
	1 : 2	7.68	0
	1 : 5	7.68	0
	1 :10	7.84	2.08
	1 : 20	7.84	2.08
	1 : 50	7.96	3.64

Table 3.46 (continued)

Ion	Se(IV) : Ion	Peak height (mV)	%Relative error
Ca^{2+}	1 : 0	7.68	0
	1 : 2	7.68	0
	1 : 5	7.68	0
	1 :10	7.76	1.04
	1 : 20	7.88	2.60
	1 : 50	7.88	2.60
Fe^{3+}	1 : 0	7.40	0
	1 : 2	7.40	0
	1 : 5	7.40	0
	1 :10	7.52	1.62
	1 : 20	7.60	2.70
	1 : 50	7.72	4.32
Zn^{2+}	1 : 0	7.40	0
	1 : 2	7.40	0
	1 : 5	7.40	0
	1 :10	7.32	-1.08
	1 : 20	7.24	-2.16
	1 : 50	7.24	-2.16
Cu^{2+}	1 : 0	7.40	0
	1 : 2	7.40	0
	1 : 5	7.60	2.70
	1 :10	7.68	3.78
	1 : 20	7.88	6.49
	1 : 50	8.20	10.81

Table 3.46 (continued)

Ion	Se(IV) : Ion	Peak height (mV)	%Relative error
Cd^{2+}	1 : 0	7.40	0
	1 : 2	7.52	1.62
	1 : 5	7.72	4.32
	1 :10	8.12	9.73
	1 : 20	8.52	15.14
	1 : 50	9.08	22.70
Cl^-	1 : 0	7.88	0
	1 : 2	7.88	0
	1 : 5	7.88	0
	1 :10	8.00	1.52
	1 : 20	8.00	1.52
	1 : 50	8.12	3.04
NO_3^-	1 : 0	7.88	0
	1 : 2	7.88	0
	1 : 5	7.88	0
	1 :10	7.88	0
	1 : 20	7.96	1.02
	1 : 50	8.04	2.03
SO_4^{2-}	1 : 0	7.88	0
	1 : 2	7.88	0
	1 : 5	7.88	0
	1 :10	7.76	-1.52
	1 : 20	7.72	-2.03
	1 : 50	7.60	-3.55

Table 3.46 (continued)

Ion	Se(IV) : Ion	Peak height (mV)	%Relative error
CO_3^{2-}	1 : 0	7.88	0
	1 : 2	7.88	0
	1 : 5	7.88	0
	1 :10	8.04	2.03
	1 : 20	8.20	4.06
	1 : 50	8.24	4.57
PO_4^{3-}	1 : 0	7.88	0
	1 : 2	7.88	0
	1 : 5	7.88	0
	1 :10	7.96	1.02
	1 : 20	8.12	3.04
	1 : 50	8.12	3.04

The experimental results obtained by investigation of some interfering species which may occur in environmental samples indicated that the presence of some interfering ions namely sodium, potassium, magnesium, calcium, iron, zinc, chloride, nitrate, sulphate, carbonate and phosphate at concentration of 50 folds that of selenite cause relative error of less than 5%. The presence of copper ions concentration up to 10 folds that of selenite, resulted in the relative error of less than 5%. While the presence of cadmium at a concentration of 5 folds that of selenite, less than 5% relative error was obtained. The presence of interfering ions was found to interfere by increasing and decreasing FIA signals. It was found that the serious positive interferences for selenite determination were cadmium and copper. Most interferences from various cations might be due to the formation of coloured complex and competitive complexation with the rhodamine dye and reagent structure contain numerous sites at which chelation with metal ions might occur that

affect absorption of complex. Ions which may oxidize iodide to triiodide under the experimental conditions, such as Cu^{2+} and ions which may form large anionic ion-complexes which can form ion-associates with rhodamine B, such as Cd^{2+}. Since interferences are many in which few interferences are significant under the optimum working conditions. Thus the method is selective and matrix effects are not severe, which can be evaluated by the method of standard additions. In addition, such high concentrations of transition-metal interferences are normally not to be expected in environmental samples.

The results as shown below (Table 3.47) showed that most effect of interfering ions on determination of selenate with photoreduction provided the similar effects on determination of selenite while some ions such as copper provided less effect than that on selenite determination.

Table 3.47 Effect of interfering ions on selenate determination.

Ion	Se(VI) : Ion	Peak height (mV)	%Relative error
Na^+	1 : 0	2.72	0
	1 : 2	2.72	0
	1 : 5	2.72	0
	1 :10	2.76	1.47
	1 : 20	2.80	2.94
	1 : 50	2.84	4.41
K^+	1 : 0	2.72	0
	1 : 2	2.72	0
	1 : 5	2.72	0
	1 :10	2.72	0
	1 : 20	2.76	1.47
	1 : 50	2.76	1.47

Table 3.46 (continued)

Ion	Se(VI) : Ion	Peak height (mV)	%Relative error
Mg^{2+}	1 : 0	2.72	0
	1 : 2	2.72	0
	1 : 5	2.72	0
	1 :10	2.76	1.47
	1 : 20	2.80	2.94
	1 : 50	2.80	2.94
Ca^{2+}	1 : 0	2.72	0
	1 : 2	2.72	0
	1 : 5	2.72	0
	1 :10	2.72	0
	1 : 20	2.80	2.94
	1 : 50	2.80	2.94
Fe^{3+}	1 : 0	3.00	0
	1 : 2	3.00	0
	1 : 5	3.00	0
	1 :10	3.00	0
	1 : 20	3.04	1.33
	1 : 50	3.04	1.33
Zn^{2+}	1 : 0	3.00	0
	1 : 2	3.00	0
	1 : 5	3.00	0
	1 :10	2.96	-1.33
	1 : 20	2.92	-2.67
	1 : 50	2.92	-2.67

Table 3.46 (continued)

Ion	Se(VI) : Ion	Peak height (mV)	%Relative error
Cu^{2+}	1 : 0	3.00	0
	1 : 2	3.00	0
	1 : 5	3.08	2.67
	1 :10	3.08	2.67
	1 : 20	3.12	4.00
	1 : 50	3.16	5.33
Cd^{2+}	1 : 0	3.00	0
	1 : 2	3.08	2.67
	1 : 5	3.20	6.67
	1 :10	3.24	8.00
	1 : 20	3.44	14.67
	1 : 50	3.64	21.33
Cl^-	1 : 0	2.60	0
	1 : 2	2.60	0
	1 : 5	2.60	0
	1 :10	2.64	1.54
	1 : 20	2.64	1.54
	1 : 50	2.68	3.08
NO_3^-	1 : 0	2.60	0
	1 : 2	2.60	0
	1 : 5	2.60	0
	1 :10	2.60	0
	1 : 20	2.64	1.54
	1 : 50	2.68	3.08

Table 3.46 (continued)

Ion	Se(VI) : Ion	Peak height (mV)	%Relative error
SO_4^{2-}	1 : 0	2.60	0
	1 : 2	2.60	0
	1 : 5	2.60	0
	1 :10	2.56	-1.54
	1 : 20	2.52	-1.54
	1 : 50	2.52	-3.08
CO_3^{2-}	1 : 0	2.60	0
	1 : 2	2.60	0
	1 : 5	2.64	1.54
	1 :10	2.64	1.54
	1 : 20	2.68	3.08
	1 : 50	2.72	4.62
PO_4^{3-}	1 : 0	2.60	0
	1 : 2	2.60	0
	1 : 5	2.60	0
	1 :10	2.64	1.54
	1 : 20	2.64	1.54
	1 : 50	2.68	3.08

3.4 Application of the Proposed Method

3.4.1 Determination of selenite and selenate in water samples

The proposed FI method was applied to speciation of selenite and selenate in water samples. The results obtained (Table 3.48) indicated that the amounts of selenite and selenate were not found in all samples which means that the contents were below the limits of detection in water samples.

Table 3.48 Determination of selenite and selenate in water samples.

Sample no.	[Se(IV)] (ppm)	[Se(VI)] (ppm)
1	ND	ND
2	ND	ND
3	ND	ND
4	ND	ND
5	ND	ND
6	ND	ND
7	ND	ND

ND = not detected

3.4.2 Comparative determination of selenite and selenate in water samples

In order to validate the proposed method for selenite and selenate determination, a comparative determination of selenate and selenite by HG-ICP-AES method was carried out. The experimental results were shown in Table 3.49. There was good agreement between the proposed FI method and the ICP method.

Table 3.49 Comparative determination of Se(IV) and Se(VI) in water samples.

Sample no.	[Se(IV)] (ppm)		[Se(VI)] (ppm)	
	FIA	ICP	FIA	ICP
1	ND	ND	ND	ND
2	ND	ND	ND	ND
3	ND	ND	ND	ND
4	ND	ND	ND	ND
5	ND	ND	ND	ND
6	ND	ND	ND	ND
7	ND	ND	ND	ND

3.4.3 Determination of selenite and selenate in spiked water samples

The proposed method was applied to spiked water samples containing selenite and selenate. The samples were analysed using the proposed method under the recommended conditions as shown in Table 3.37. The results are presented in Table 3.50. The experimental results obtained with good percentage recoveries which means that the proposed method is suitable for the determination of selenite and selenate in the sample solutions. From the experimental results, the difference in recoveries for the samples could be due to different chemical compositions of water samples which collected from different locations.

Table 3.50 Determination of selenite and selenate in spiked water samples using the proposed procedure.

Sample no.	[Se(IV) (ppm)]			[Se(VI)] (ppm)		
	Added	Found	%recovery	Added	Found	%recovery
1	0.010	0.010	100	0.010	0.009	90.0
2	0.050	0.050	98.0	0.050	0.048	96.0
3	0.100	0.097	97.0	0.100	0.105	105
4	0.300	0.305	102	0.300	0.275	91.7
5	0.500	0.492	98.4	0.500	0.510	102
6	0.700	0.723	103	0.700	0.695	99.3
7	1.000	0.995	99.5	1.000	0.926	92.6